NRL Report 7142
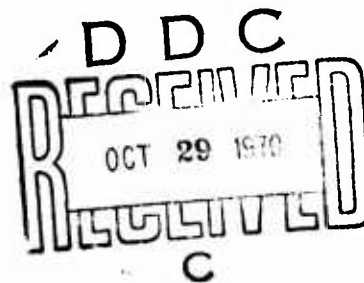
Radar Sea Return in High Sea States

J. C. DALEY, W. T. DAVIS, AND N. R. MILLS

*Wave Propagation Branch
Electronics Division*

September 25, 1970

DDC

RECEIVED

OCT 29 1970

C

NAVAL RESEARCH LABORATORY
Washington, D.C.

CONTENTS

ABSTRACT

In order to obtain a more exact specification of the variation of the radar cross section of the sea with increasing sea roughness, and to determine a worst-case condition for sea clutter, NRL has conducted a high-sea-state clutter measurement program in the North Atlantic.

The processing and analysis of the radar backscatter, recorded in the North Atlantic in February 1969, have been completed. Radar return was collected on four frequencies in both linear and cross polarizations, and the normalized radar cross section σ_0 of the sea surface was obtained as a function of radar and surface parameters for the high sea states encountered. The study of the behavior of the median value of σ_0 as a function of the radar parameters and sea conditions resulted in the following conclusions at high sea states characterized by winds of 20-50 knots and wave heights of 10-26 ft: (a) the value of σ_0 is independent of wavelength for vertical polarization but maintains an inverse wavelength dependence for horizontal polarization, (b) the direct polarization ratio remains significant for all wavelengths as the sea roughness increases and is a function of wavelength, (c) the value of σ_0 is sensitive to wind direction, with consistently higher clutter observed in the upwind direction for all wavelengths and both direct polarizations, and (d) the value of σ_0 does not increase significantly with wind velocity in the region 20-50 knots, indicating that σ_0 approaches a maximum value, or "saturation," with increasing surface roughness. The high-sea-state measurement program has provided a comprehensive data of pulse-to-pulse returns which may be analyzed to develop statistical models of the sea clutter process.

PROBLEM STATUS

RADAR SEA RETURN IN HIGH SEA STATES

INTRODUCTION

In the past few years, considerable interest has developed in the behavior of radar sea return (clutter) in the higher sea states, i.e., those with wind speeds in excess of 20 knots and wave heights in excess of 10 ft. Prior to this time, the radar return at shallow grazing angles (less than 45°) had been assumed (1) to increase with surface roughness until a saturation condition was reached in which the radar cross section (RCS) of the sea became slowly varying and, in effect, constant. Four-frequency radar (4FR) measurements (2) in Beaufort wind fields from zero through four in the vicinity of Puerto Rico in 1965 tend to confirm this hypothesis without, however, proving the existence of the saturation condition. With the advent of system designs for long-range ocean surveillance radars, whose performance is critically dependent on the sea return background, as well as the development of remote sensors using active radar to determine sea state and wind velocity, a more exact specification of the variation of the RCS of the sea with increasing roughness was required to define the boundaries of the saturation region or, in lieu of this, to determine a worst-case condition for the sea return.

To satisfy such requirements a measurement program was planned to document the behavior of the sea return in such high sea states under conditions in which sufficient surface truth was available to specify growth characteristics of the RCS with wind and wave height, as well as to provide the sea-state conditions under which saturation of the cross section, if it existed, would occur. In order to achieve these objectives, a measurement site was selected at which the probability of observing rough seas was high, and simultaneously, where a source of surface truth could be obtained, to specify the experiment. This site was found in the North Atlantic Ocean where in the winter months a storm flow, shown in Fig. 1, proceeds south of Labrador, Greenland, and Iceland across the ocean and along the European coast. As a result, during January and February, there is a 30% probability of wave heights in excess of 12 ft and a 10% probability of wave heights in excess of 20 ft. In the path of these storms, as shown, are ocean stations "I" (India, 59°N, 19°W) and "J" (Juliet, 52.5°N, 20°W), on which oceanographic surface vessels (OSV), staffed and maintained by the British, Dutch, and French weather services, are located on a rotating schedule. These vessels not only provide oceanographic and meteorological observations to the International Weather Services, but they also are equipped with radio beacons to serve as check points for transoceanic flights and, consequently, are almost ideal terminal points for the measurement program.

In February 1969, the 4FR System was deployed to Shannon, Ireland, and during the first three weeks of the month, nine missions were flown either to ocean station India or Juliet. The choice of site was made on a basis depending on the sea state reported by each station and the meteorological forecast. At the station, the OSV was used as a reference point and the flight plan shown in Fig. 2 was initiated. The plan consists of three legs flown in upwind, downwind, and crosswind directions at each of three altitudes, and a tenth leg flown on the return to Shannon.

The use of three altitudes in the flight program is necessitated by the difficulty of encompassing the entire dynamic range of the sea return, as a function of antenna depression angle, in the radar receiver since gain settings must remain constant to maintain calibration. The altitudes shown in Fig. 2 are nominal. The lower altitude was
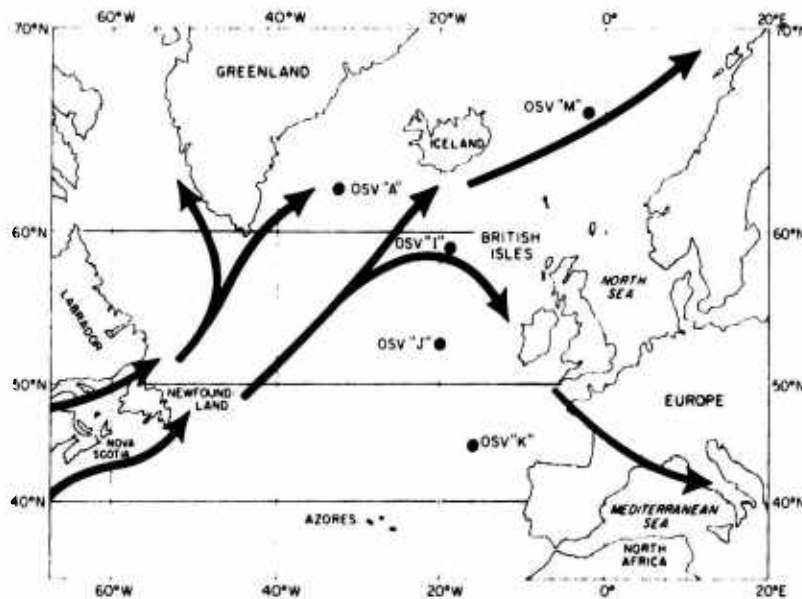
1

Fig. 1 - Prevailing storm tracks during the winter season over
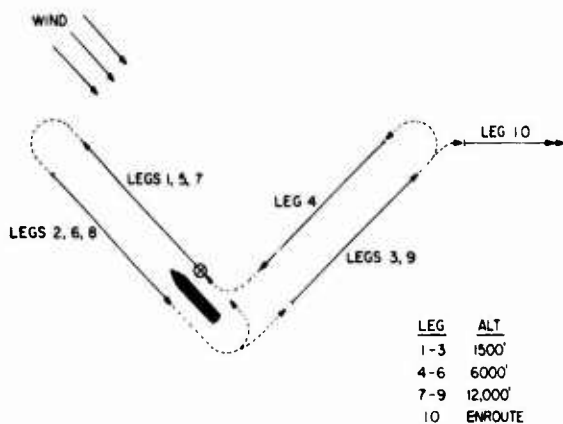the North Atlantic Ocean

Fig. 2 - Aircraft flight pattern
which was followed when col-
lecting radar data at each of
the oceanographic surveillance
stations

LEG	ALT
1-3	1500'
4-6	6000'
7-9	12,000'
10	ENROUTE

primarily set by visibility of the ocean surface as required by the aerial cameras and
laser altimetry. On the low-altitude legs, data were taken on leg 1 (upwind) at shallow
grazing angles from 5° through 30° by fixing the antenna depression angle (the azimuth
angle was along the flight path) and recording the return over approximately a 40-sec
period, resetting at the next depression angle in the sequence, and repeating the proce-
dure until the angular range was covered. The antenna was then rotated 180° in azimuth
and the same range of depression angles set and the return measured. This enabled up-
wind, downwind, and data in both directions across the wind to be acquired on each leg.
After the upwind leg, a downwind leg and crosswind leg were flown with a repetition of
the measurement procedure. On the medium-altitude legs, data were collected in a
similar manner at grazing angles from 20° to 60° where the angular overlap provided a
measure of the constancy of the cross section with altitude and time. A similar over-
lapping of angles was performed at the higher altitude, where the angle varied from 60°
to 90° (normal incidence).

Generally the measurement program commenced at 1300Z, and the entire pattern required approximately 2 to 3 hr to finish, depending on wind speed. The tenth leg shown in Fig. 2 was flown on the return at a constant altitude to evaluate the variation of the cross section in a varying sea condition.

Table 1 lists, on an hourly basis, the wind and wave conditions which were reported at the ocean stations for each mission. As can be seen, on seven of the nine missions, data were acquired in sea states in which the wind exceeded 20 knots—which was the largest wind condition observed in the Puerto Rico experiment. The maximum-sea-state condition was observed on February 11 when a 26-ft wave height was combined with a 46-48 knot wind. As will be noted at a later point, this maximum sea condition which occurred under blue skies does not provide the maximum values of the cross section. These values occurred on February 6 when there were intermittent snow falls over the measurement area. Unfortunately, little data have been obtained at this time to document the wind variation on this day beyond that listed, and verbal reports on the site indicated gusty conditions which could have produced a stronger wind field later in the day. However, in view of the variation of the cross section with wind exhibited during the remainder of the experiment, the increase in cross section is primarily attributed to the presence of the precipitation.

Before continuing with the results of the high-sea-state measurement program, a brief review of the 4FR System will be undertaken since its characteristics impose constraints on the cross-section measurements which must be considered in the interpretation of the data.

THE MEASUREMENT SYSTEM

The 4FR System is an airborne, coherent, pulsed radar which is capable of transmitting a sequence of four frequencies alternately on horizontal and vertical polarization. These frequencies are X band (8910 MHz), C band (4455 MHz), L band (1228 MHz), and P band/UHF (428 MHz). The dual polarized operation is achieved by switching the transmitters between horizontally and vertically polarized feeds in the antenna system. The 4FR antenna system is composed of four antennas which are mounted in pairs, back to back. One pair, the X- and C-band antennas, are circular parabolas which have a common boresite and have equal beamwidths so that they illuminate equal areas. The other pair, the L- and P-band antennas, are intermixed crossed dipole arrays with a common boresite but unequal beamwidths so that the area illuminated by the P-band antenna includes that illuminated by the L-band antenna. In operation, the 4FR System alternates its transmissions in the sequence shown in Fig. 3. The minimum period τ of the alternations is 170 μs, while the period T for any frequency/polarization combination is 1.27 ms.

The receiving system of the radar is designed to detect both the directly polarized return, e.g., the horizontally polarized return from a horizontally polarized transmission (HH), and the cross polarized return, e.g., the vertically polarized return from a horizontally polarized transmission (HV). Consequently, sixteen variables are present in the receiving sequence, four for each frequency. These four are the complex components of the scattering matrix and offer a nearly complete description of the reflection characteristics of targets over the parameter range to a limit determined by the resolution cell of the radar. The receiver has two channels, one for horizontally polarized returns and the other for the vertically polarized. These channels function to preserve the amplitude and phase of each component and are time shared by the transmitters so that calibration is simplified by eliminating relative drift errors. The amplitude and phase are measured independently in each channel. In the amplitude measurement, the signal is first logarithmically amplified to compress the dynamic range and then incoherently detected. In the phase measurement, on the other hand, the signal is first amplified

Table 1
Gross Surface Conditions High-Sea-State Program

		1200Z		1300Z		1400Z		1500Z		1600Z	
		Waves	Wind	Waves	Wind	Waves	Wind	Waves	Wind	Waves	Wind
6 FEB. 'T'	Sea			14.8',9sec	340/40						
	Swell			23',13sec 330°							
8 FEB. 'J'	Sea	2',3sec	160/09	2',3sec	080/07	2',3sec	CALM			2',3sec	110/06
	Swell	11.5',9sec 330°		11.5',9sec 330°		11.5',9sec 330°				14.8',9sec	
10 FEB. 'T'	Sea			11.5',7sec	240/31	13.1',10sec	240/33	13.1,8sec	240/30	13.1',8sec	240/35
	Swell			18',10sec 260°		18',10sec 240°		18',10sec 240°		18',10sec 240°	
11 FEB. 'T'	Sea	21.3',10sec	290/46	21.3',10sec	290/46	21.3',10sec	290/48	21.3',10sec	290/48	23',10sec	290/52
	Swell	26.2',12sec 280°		26.2',12sec 280°		26.2',12sec 280°		26.2',12sec 280°		29.5',12sec 280°	
13 FEB. 'J'	Sea	23',12sec	360/39	23',12sec	360/35	23',12sec	360/35	23',12sec	350/39	23',12sec	360/37
	Swell										
14 FEB. 'J'	Sea	23',10sec	101/38	26.2',10sec	101/40	26.2',10sec	101/40	23',12sec	360/37		
	Swell										
17 FEB. 'T'	Sea	3',3sec	290/08	3',3sec	240/05	3',1sec	260/05	3',1sec	250/05	0 Sea	CALM
	Swell	9.8',7sec 240°		11.5',7sec 240°		11.5',7sec 240		11.5',7sec 240°		9.8',6sec 240°	
18 FEB. 'J'	Sea	9.8',10sec	110/22	9.8',10sec	110/22	11.5',10sec	100/22	11.5',10sec	120/26	11.5',8sec	110/22
	Swell										
20 FEB. 'J'	Sea			16.4',10sec	060/29	16.4',10sec	060/29	16.4',10sec	050/28		
	Swell										
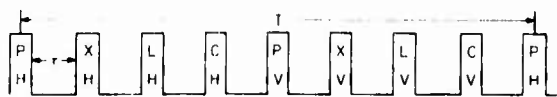
4FR TRANSMISSION SEQUENCE

Fig. 3 - Transmission and re-
ception Radar sequences used in
the four-frequency radar (4FR)
system
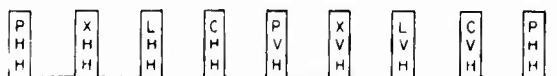
4FR RECEPTION SEQUENCE

and hard limited at an intermediate frequency (i-f) to eliminate amplitude fluctuations
and then coherently detected using a stored reference. All signals are gated in range by
an operator, digitized to 7-bit accuracy, and recorded in flight for later analysis.

Some of the system characteristics of the 4FR System are given in Table 2. A
more detailed description of the system is given by Guinard (3). The 4FR System allows
many choices of pulse repetition frequency (prf), pulse length, i-f bandwidth, and range
gate width. The values used for these parameters during this program were prf, 683,
from February 6 to 11, and 603 from February 13 to 20; pulselength, 0.5 μs; i-f band-
width, 10 MHz; and range gate width, 24 ns.

Table 2
4-Frequency Radar System Parameters

Parameter	P - Band		L - Band		C - Band		X - Band	
Polarization	Horiz	Vert	Horiz	Vert	Horiz	Vert	Horiz	Vert
Az. Beamwidth	±12. 3°	12. 1	5. 5°	5. 5°	5°	5°	5°	4. 7°
El. Beamwidth	40°	41	13. 8°	13	5°	5°	5. 3°	5. 0°
Az. Minor Lobe (dB)	14. 5	14. 5	13. 4	14	23. 2	23. 2	23. 6	23. 6
El. Minor Lobe (dB)	30	26.	16	14	24. 5	24. 5	23. 5	24. 2
Cross Pol. (dB)	25	28	25	25	>20	>20	>20	>20
Antenna Gain (dB)	17. 4	17. 4	25. 9	26. 2	31. 4	31. 4	31. 2	31. 2
Peak Power (kW)	25		25		35		25	
Av Power (W)	140		140		100		160	
Pulse Width (..s)	0. 25 - 2. 0		0. 25 - 2. 0		0. 1 - 2. 0		0. 1 - 2. 0	
PRF	100 - 1463 pps		100 - 1463 pps		100 - 1463 pps		100 - 1463 pps	

One of the major problems involved in the measurement of cross section from an airborne platform is the calibration of the radar system. In general, two calibrations are required to eliminate system constants. The first is an internal calibration which is accomplished by measuring the receiver transfer function from the antenna output terminals to the recording medium by means of standard signal generators. The second is an external calibration to determine the constants related to the antenna gain, radome losses, radiated power, and system losses. In the latter measurement, 8-in. aluminum spheres are used as reference targets of known cross section. These are dropped from the aircraft and tracked manually. Figure 4 is an example of the sphere measurement. The ordinate in this figure is relative amplitude of the return, in decibels, and the abscissa is the range plotted on a logarithmic scale. The figure is a compilation of several sphere tracks made consecutively prior to the measurement of the sea return on February 14, 1969. Each point represents the upper-decile value of a thirty-two-pulse sample of the return. The upper decile is used to estimate the maximum value of the return since all errors in sphere tracking tend to lower the observed values of the cross section.
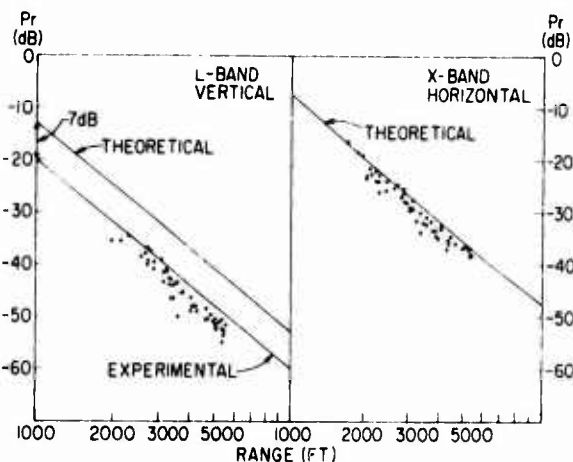

Fig. 4 - Measured and calculated radar returns from 8-in. aluminum spheres used as reference targets for the external calibration of the 4FR System

The indicated theoretical maximum value of the return is computed from the radar equation using the measured transmitter power, the value of the cross section, the antenna gain appropriate for the frequency transmitted, and an estimate of the line and radome losses. As can be seen in the X-band horizontal case, the theoretical value provides an excellent measure of the calibration value for the return. On the other hand, the L-band vertical case shows a 7-dB loss between the theoretical maximum value and the sphere return, indicating the presence of other losses in the system not accounted for in the theoretical calculation. In order to use this calibration procedure effectively, all cross-section values are referenced to the measured sphere cross section in the following manner. The RCS of the sphere is given by

$$\sigma_S = \frac{(4\pi)^3}{G^2 \lambda^2} \frac{P_{rS}}{P_{TS}} R_S^4 \tag{1}$$

where P_{rS} and P_{TS} are the received and transmitted powers, respectively, λ is the radar wavelength, G is the maximum antenna gain, and R_S is the range to the sphere. Applying the same definition to the target cross section σ_T and taking the ratio of σ_T to σ_S gives

$$\sigma_T = \frac{P_{r\,T}}{P_{r\,S}} \left(\frac{R_T}{R_S}\right)^4 \sigma_S \tag{2}$$

where σ_T is the target cross section and $P_{r\,T}$ is the corresponding radar return. In the presence of sea clutter, the normalized radar cross section is defined by

$$\sigma_0 = \frac{\sigma_T}{A} \tag{3}$$

where A is the illuminated area. Then the radar equation for clutter becomes

$$\sigma_0 = \frac{P_{r\,T}}{P_{r\,S}} \left(\frac{R_T}{R_S}\right)^4 \frac{\sigma_S}{A} \tag{4}$$

where the peak power is the same for both measurements. The sphere terms in Eq. 4 are determined by the in-flight measurement, and the illuminated area A is calculated from the geometry of the data run. At small (near-horizontal) incident angles, the area is pulse-length limited and is approximated by

$$A = R_T \ell_a \frac{1}{2} \frac{c\tau}{\cos\theta} \tag{5}$$

where ℓ_a is the azimuth beamwidth between the half-power points of the return signal, τ is the pulse length, and θ is the incident angle. At large angles, when the area is beamwidth limited, A is approximated by

$$A \quad R_T^2 \frac{\ell_a \ell_e}{\sin\theta} \tag{6}$$

where ℓ_e is the elevation beamwidth between half-power points.

The above procedure is used to calibrate all eight direct-polarization components in flight on each mission. The eight cross-polarization components are calibrated by the appropriate direct measurement, e.g., at the X-band frequency X_{VH} is calibrated by X_{HH}.

In addition to the sphere measurement, and in view of the many switching operations involved in the 4FR System, a constant fraction of the transmitted power, termed the reentrant signal, is inserted into each of the microwave input lines and observed at the operator's console to monitor system performance. The reentrant signal is periodically recorded with the data to assess system stability. As a result of these calibration procedures, a typical cross-section accuracy of ±2 dB is achieved. This value is obtained by monitoring receiver drift and noting the scatter of measurements of the reference sphere when illuminated under optimum conditions.

DATA PROCESSING

Since radar clutter is a statistical process, the random return is best described by its probability distribution. The calculation of the distribution is accomplished through the use of a small, general purpose, digital computer which accepts the raw range samples and is suitably programmed to both calibrate the data and provide the desired parameters. The basic outputs of the processing system are cumulative probability

distributions of the received power (in decibels) of the sixteen possible frequency-
polarization amplitude components recorded by the 4FR System over the total recording
period ($\approx$ 40 s). Sample plots are shown in Figs. 5a through c. The distribution has
been plotted versus a normal probability scale in Figs. 5a and b and versus a Rayleigh
probability scale in Fig. 5c. In the first case, a log normal distribution would be plotted
as a straight line. In the second case, a Rayleigh distribution would be plotted as a
straight line of a given slope. The plots show the general results observed, namely,
that the distribution of clutter varies between log normal and Rayleigh. The coding in
the upper left of each plot indicates the date, run, and signal component, e.g., for Figs.
5a-c, Run 141, L_{HH}; Run 77, P_{VV}; and Run 53, X_{HH}, respectively. Through the sphere
measurement, the received power (in dB) may be calibrated in terms of the normalized
RCS (σ_0) as defined previously. The median value of σ_0 was read from these plots (+4.5
dB in Fig. 5a) and tabulated for all sixteen signal components for each data run. During
the nine missions flown over the North Atlantic, over 800 such data runs were recorded
in addition to the necessary calibration procedures described previously. For each mis-
sion, median σ_0 values of these runs were grouped according to wind direction and angle
for each signal component. The median of these sample medians was computed and
tabulated for each mission. The results for the direct polarizations are listed in Tables
3 through 10, and the cross polarizations in Tables 11 through 18, with the appropriate
wind field and wave height observed during the radar measurement period. The total
sample generally included from 2 to 4 data runs (80 to 100 s). The RCS values are
given for upwind, downwind, and crosswind conditions for all angles except 75° and 90°.
At these angles, all the reliable data were combined without regard to wind direction,
since antenna pointing errors from run to run could be larger than the expected variation
due to wind direction. Omissions in the tables are due to minor problems resulting in
lack of data for that particular case, especially at 5° where the signal on some wave-
lengths was below the minimum detectable radar return. All data taken on February 8,
1969, are omitted because equipment problems resulted in unreliable sphere measure-
ments and, therefore, absolute calibration of the data was not possible.

DEPENDENCE OF σ_0 ON RADAR PARAMETERS

In accordance with the flight plan described previously, sea return was recorded as
a function of antenna depression angle for settings of 5, 10, 20, 30, 45, 60, 75, and 90°.
Curves of σ_0 versus angle for each missions are shown in Fig. 6 for VV polarized data
and in Fig. 7 for HH polarized data both in the upwind direction. The angular variation
of σ_0 conforms to previous experimental results (1, 2). In addition, a recent model, based
on slightly rough scattering, approximates the angular dependence of σ_0 for angles away
from normal incidence. The model is based on a composite rough surface, with smaller
scattering elements riding on the larger swell structure. It has been shown by Wright (4)
that the effective backscattering elements from the sea surface are the Bragg resonant
waves, i.e., waves of length L (λ 2) sec , where λ is the radar wavelength and is
the grazing angle. An extension of this model, introducing polarization effects, has
been accomplished by Valenzuela (5). The predicted σ_0 versus relationships have
been published previously (6) and are included in the Appendix with the details of compu-
tation. Similar data are plotted for the cross-polarized case (VH) in Fig. 8. For the
moderate angle region from 20° to 60°, σ_0 increases at a slower rate for cross
polarization.
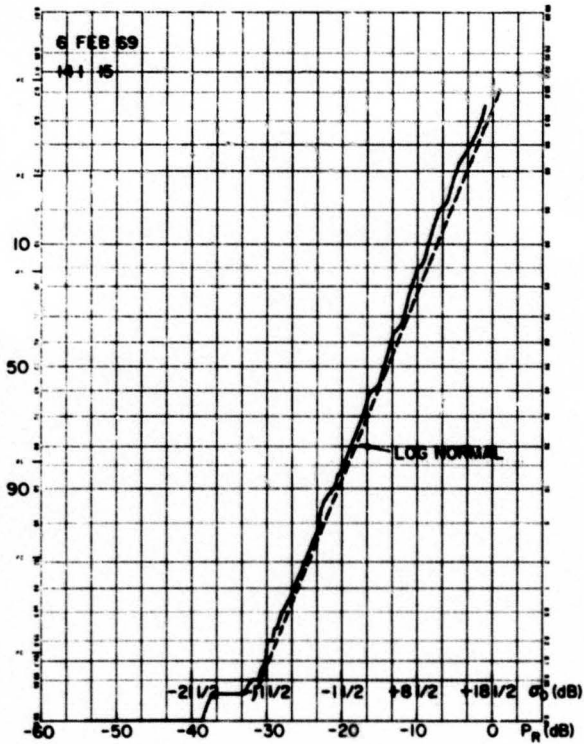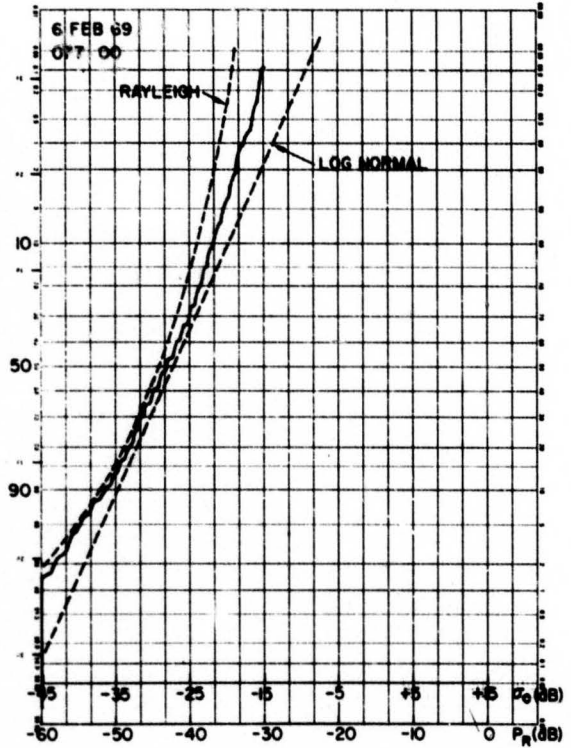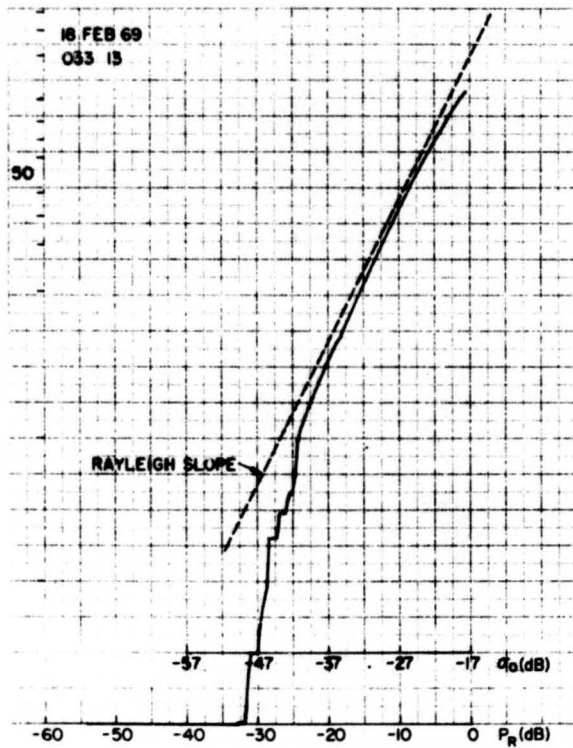
Fig. 5 – Samples of cumulative probability distributions for received radar signal power P_R compared to a normal distribution (a and b) and a Rayleigh distribution (b and c)

DALEY, DAVIS, AND MILLS

Table 3
Median Values of the Normalized Radar Cross Section σ_0 for Directly
Polarized Signals Measured at X, C, L, and P Bands

Feb. 6, 1969: Wind Velocity 40 knots; Wave Height 15 ft.

Depression Angle (degrees)	Wind Direction*	σ_0 (dB)							
		X_{VV}	X_{HH}	C_{VV}	C_{HH}	L_{VV}	L_{HH}	P_{VV}	P_{HH}
5	U	-34.5	-39	-35	-43	—	—	-37	-43
	D	-34.5	-40	-35	-43	—	—	-37.5	-42
	C	-34	-35	-36	-39.5	—	—	-40.5	-44.5
10	U	-28.5	-32	-28	-36	—	—	-30.5	-40.5
	D	-29.5	-34	-30	-38.5	—	—	-29	-39
	C	-30.5	-35.5	-32.5	-39	—	—	-33	-41
20	U	-24.5	-27.5	-24	-32	-23	-33.5	-24	-41.5
	D	-27	-35	-27	-40	-24	-37	-25.5	-39
	C	-29.5	-35.5	-31	-40	-25.5	-38	-28.5	-43.5
30	U	-21	-26.5	-21.5	-29	-21.5	-29	-25	-31.5
	D	-23.5	-30	-23.5	-32	-22.5	-32.5	-23.5	-31.5
	C	-25	-30.5	-25.5	-34	-22	-32	-27.5	-35
45	U	-18.5	-19.5	-17	-22	-19.5	-24.5	-22	-25
	D	-19	-22	-18	-24.5	-20	-26	-21.5	-25.5
	C	-22.5	-24.5	-21	-27.5	—	—	-25	-28.5
60	U	-14	-14.5	-14.5	-15.5	-14	-17.5	-17.5	-17
	D	-13.5	-16	-14.5	-17.5	-16	-19.5	-18	-17.5
	C	-17	-18	-16.5	-20	-18	-21	-19.5	-19.5
75	—	-8	-6.5	-5.5	—	-2.5	-3	-10.5	-9.5
90	—	+3	+2	+6.5	—	+7	+4.5	+4.5	+5

* U = upwind, D = downwind, and C = crosswind.

Table 4
Median Values of the Normalized Radar Cross Section σ_0 for
Directly Polarized Signals Measured at X, C, L, and P Bands

Feb. 10, 1969: Wind Velocity 30-33 knots; Wave Height 11.5-13.1 ft.

Depression Angle (degrees)	Wind Direction*	σ_0 (dB)							
		X_{VV}	X_{HH}	C_{VV}	C_{HH}	L_{VV}	L_{HH}	P_{VV}	P_{HH}
5	U	-36	-38			-35.5	-44	-41	-52
	D	-34.5	-40.5			-42	-53	-44.5	-55.5
	C	-37	-40			-40.5	-48.5	-44.5	-54.5
10	U	-32.5	-35.5			-31.5	-43	-36.5	-44.5
	D	-34	-40			-35	-51	-37.5	-50.5
	C	-35	-39.5			-34.5	-47.5	-37.5	-48.5
20	U	-29.5	-32			-26	-38	-27.5	-46
	D	-30.5	-35.5			-30	-44	-30	-49
	C	-29.5	-36.5	NOT RECORDED		-29	-42	-31.5	-49
30	U	-26	-31.5			-24.5	-34	-30	-37.5
	D	-26	-31.5			-27	-38.5	-31	-41
	C	-26.5	-32.5			-26	-37.5	-31	-39.5
45	U	-23	-23			-21.5	-27	-25	-29
	D	-23.5	-24			-23.5	-30.5	-27	-31.5
	C	-24.5	-25.5			-23	-29.5	-26.5	-31
60	U	—	-17.5			-17.5	-20	-22	-22.5
	D	—	-21.5			-19.5	-22	-23	-24
	C	—	-19			-20	-22	-23	-24
75	—	-11	-10.5			—	—	-11	-13.5
90	—	-3	-0.5			—	—	0	+0.5

* U = upwind, D = downwind, and C = crosswind.

Table 5
Median Values of the Normalized Radar Cross Section σ_0 for
Directly Polarized Signals Measured at X, C, L, and P Bands

Feb. 11, 1969: Wind Velocity 46-48 knots; Wave Height 21.3 ft.

Depression Angle (degrees)	Wind Direction*	σ_0(dB)							
		X_{VV}	X_{HH}	C_{VV}	C_{HH}	L_{VV}	L_{HH}	P_{VV}	P_{HH}
5	U	-36.5	-36	-36.5	-40.5	-34.5	-42.5	-40.5	-48
	D	-33.5	-37	-32.5	-42.5	-37.5	-50	-44	-55.5
	C	-35.5	-36	—	—	-38	-45.5	-46	-52.5
10	U	-31.5	-35	-29	-38	-27	-39	-33.5	-41.5
	D	-30	-35	-27	-40	-30	-47.5	-37	-50
	C	-31.5	-34.5	—	—	-32.5	-44.5	-39.5	-49
20	U	-26.5	-30.5	-25	-34.5	-22.5	-36.5	-29	-46.5
	D	-28	-33	-26	-36.5	-26	-42	-31	-48.5
	C	-29	-35	-29.5	-37.5	-28	-42	-34.5	-49
30	U	-24	-28	-22	-30	-22	-32	-27.5	-35
	D	-27	-31.5	-24.5	-34.5	-21	-36	-28.5	-38.5
	C	-27.5	-32	-25.5	-34.5	-25.5	-36.5	-32.5	-40
45	U	-20.5	-23	-20.5	-26	-19	-25	-25	-28
	D	-20.5	-24	-21.5	-27.5	-20.5	-30	-26	-31.5
	C	-23	-24.5	-23.5	-29.5	-23	-30.5	-29	-33.5
60	U	-16	-16.5	-17	-18.5	-14	-17	-21.5	-21.5
	D	-16.5	-17.5	-18	-21	-15.5	-20.5	-23	-24
	C	-19	-20	-19.5	-23	-17.5	-21.5	-24	-24.5
75	—	-8	-8	-6	—	-5.5	—	-12	-14
90	—	-1	-2	+2	-1.5	—	—	-4	-4.5

* U = upwind, D = downwind, and C = crosswind.

Table 6
Median Values of the Normalized Radar Cross Section σ_0 for
Directly Polarized Signals Measured at X, C, L, and P Bands

Feb. 13, 1969: Wind Velocity 35-39 knots; Wave Height 23 ft.

Depression Angle (degrees)	Direction*	σ_0 (dB)							
		X_{VV}	X_{HH}	C_{HH}	C_{VV}	L_{VV}	L_{HH}	P_{VV}	P_{HH}
5	U	-37	-37.5	-36.5	-40	-35.5	-42	-40	-48
	D	-36.5	-40	-35	-42	-40	-49.5	-42.5	—
	C	-38.5	-39.5	-38	-41.5	-42	-46	-44	-51
10	U	-33.5	-35.5	-31	-39	-30.5	-43	-34	-46
	D	-31.5	-39	-30.5	-43	-34	-47.5	-36	-50
	C	-33.5	-37	-32.5	-41	-35	-46.5	-37	-49
20	U	-28	-32.5	-26.5	-35	-25	-36.5	-28	-45
	D	-28	-36	-27	-39	-28	-42	-29.5	-49.5
	C	-30	-34	-30	-38.5	-30.5	-41.5	-32	-48
30	U	-25.5	-29.5	-24	-32	-23	-31.5	-26	-35.5
	D	-26	-31.5	-25	-34	-27.5	-38	-28.5	-39
	C	-29.5	-34	-28	-37	-28	-37	-30	-39.5
45	U	-21	-22	-19.5	-25	-20.5	-25	-23.5	-27.5
	D	-21.5	-23.5	-21	-27	-23.5	-29.5	-24.5	-31
	C	-24.5	-26	-24.5	-30	-25.5	-30.5	-26	-32
60	U	-17	-16.5	-16	-17.5	-15.5	-17	-19	-21
	D	-19.5	-19.5	-19	-21.5	-17.5	-18.5	-20	-22
	C	-19.5	-18	-20.5	-21.5	-19.5	-20.5	-21	-22.5
75	—	-8.5	-6.5	-7	-9	-6	-8	-8.5	-12
90	—	-2.5	-1	0	0	-2	-3.5	+4.5	+3.5

* U = upwind, D = downwind, and C = crosswind.

DALEY, DAVIS, AND MILLS

Table 7
Median Values of the Normalized Radar Cross Section σ_0 for
Directly Polarized Signals Measured at X, C, L, and P Bands

Feb. 14, 1969: Wind Velocity 37-40 knots; Wave Height 23-26 ft.

Depression Angle (degrees)	Wind Direction*	σ_0 (dB)							
		X_{VV}	X_{HH}	C_{VV}	C_{HH}	L_{VV}	L_{HH}	P_{VV}	P_{HH}
5	U	-37	-37.5	-34	-41.5	-36	-44.5	-41.5	-46.5
	D	-35.5	-40.5	-33.5	-46	-41.5	—	-44	—
	C	—	—	-38.5	-42.5	-43.5	-49.5	-45	—
10	U	-32.5	-35.5	-29.5	-39	-31	-43.5	-36	-46
	D	-32	-37	-29.5	-43	-36.5	-52.5	-38.5	-50.5
	C	—	—	-34.5	-42.5	-36.5	-48.5	-38	-50.5
20	U	-27.5	-32	-26	-35.5	-25.5	-39	-29	-44.5
	D	-28.5	-34.5	-25.5	-37.5	-29.5	-44.5	-31	-49
	C	-30.5	-36	-31	-40	-32.5	-45	-33.5	-47
30	U	-25.5	-29.5	-23.5	-31.5	-24	-33	-27.5	-35
	D	-27	-33	-25	-36	-27	-39	-29.5	-39
	C	-28	-32.5	-29.5	-38.5	-29.5	-39	-32.5	-40.5
45	U	-21	-22.5	-21	-26	-22.5	-27.5	-25.5	-29
	D	-21.5	-24.5	-21.5	-28	-24	-30	-26	-31
	C	-24	-26.5	-25	-30	-28	-33.5	-29	-32.5
60	U	-17	-17	-16	-18	-17	-19	-21.5	-22.5
	D	-17	-18	-17	-20	-18.5	-20.5	-22	-23.5
	C	-19	-19.5	-19.5	-22	-20.5	-21.5	-23.5	-23
75	U	-9.5	-9.5	-7.5	-10.5	—	—	-15.5	-17
90	—	-1	+0.5	+3.5	+2	—	—	-1	+0.5

* U = upwind, D = downwind, and C = crosswind.

Table 8
Median Values of the Normalized Radar Cross Section σ_0 for
Directly Polarized Signals Measured at X, C, L, and P Bands

Feb. 17, 1969: Wind Velocity 5 knots; Wave Height 3 ft.

Depression Angle (degrees)	Wind Direction*	σ_0(dB)							
		X_{VV}	X_{HH}	C_{VV}	C_{HH}	L_{VV}	L_{HH}	P_{VV}	P_{HH}
5	U	-48.5	-46	-44.5	-50.5	-44.5	—	-45.5	—
	D	-48.5	-49.5	—	—	-43.5	—	-44	—
	C	-47.5	-47.5	-49.5	-53	-44.5	—	-45	—
10	U	-46.5	-46.5	-42.5	-49.5	-37	-54.5	-38	-55
	D	-46	-54.5	-43.5	-58.5	-36	-54	-37.5	-54
	C	-43	-50.5	-40.5	-53.5	-37.5	-55	-36.5	-54.5
20	U	-45	-48.5	-40	-53	-34	-47	-30.5	-52
	D	-42.5	-48.5	-38	-53	-31.5	-46	-29.5	-51.5
	C	-38	-44.5	-35.5	-46.5	-31.5	-46.5	-31	-50.5
30	U	-41	-46.5	-38	-47.5	-31	-41.5	-30.5	-41
	D	-39.5	-46.5	-36	-47.5	-29	-40.5	-29.5	-40
	C	-35.5	-43.5	-33.5	-44	-30	-40	-28.5	-40
45	U	-36	-38.5	-31	-38.5	-27	-33.5	-26.5	-33.5
	D	-34.5	-38.5	-30.5	-38	-26	-32.5	-25.5	-33.5
	C	-33.5	-37	-29	-36.5	-27	-34	-26	-31.5
60	U	-26	-26.5	-22.5	-26	-20	-21.5	-22	-25.5
	D	-25.5	-25	-22	-26	-19.5	-21	-21.5	-24.5
	C	-24.5	-24.5	-21.5	-25	-20	-21	-20.5	-23.5
75	–	-12	-12	-8	-12	—	—	-14.5	-16
90	–	+1.5	+1.5	+6	+3.5	—	—	+5	+4

* U = upwind, D = downwind, and C = crosswind.

Table 9
Median Values of the Normalized Radar Cross Section σ_0 for
Directly Polarized Signals Measured at X, C, L, and P Bands

Feb. 18, 1969: Wind Velocity 22 knots; Wave Height 9.8 ft.

Depression Angle (degrees)	Wind Direction*	σ_0(dB)							
		X_{VV}	X_{HH}	C_{VV}	C_{HH}	L_{VV}	L_{HH}	P_{VV}	P_{HH}
5	U	-38	-40.5	-38	-41.5	-41.5	-47	-45	-49
	D	-39.5	-44	-40.5	-43	-42	-49.5	-44.5	-49.5
	C	-41.5	-40.5	-45	-42.5	-42.5	-48	-44	-49.5
10	U	-34.5	-39	-34.5	-42.5	-33	-46	-37.5	-46.5
	D	-34.5	-44	-34.5	-46	-36.5	-52.5	-39	-50.5
	C	-37.5	-41	-40.5	-44.5	-36.5	-50.5	-38.5	-52
20	U	-30.5	-36.5	-31	-39	-28.5	-41.5	-31	-46
	D	-31	-40	-31	-41.5	-30.5	-45	-31	-48
	C	-35	-40	-36.5	-42.5	-31.5	-44.5	-31	-45.5
30	U	-27.5	-33	-27.5	-36.5	-25.5	-36	-29.5	-36
	D	-29	-37	-28.5	-39.5	-28	-38.5	-31	-37.5
	C	-33.5	-39	-35	-41	-30	-40	-31	-37.5
45	U	-22	-25	-23	-28.5	-22.5	-28.5	-26.5	-30
	D	-23	-27	-24	-30.5	-26	-33.5	-28	-31
	C	-28.5	-31	-29.5	-34	-26.5	-32.5	-27.5	-32
60	U	-18.5	-18.5	-20	-22	-17.5	-19.5	-21.5	-22
	D	-19.5	-20.5	-19.5	-22.5	-19	-21	-22	-22.5
	C	-25.5	-24.5	-25	-26	-20.5	-22.5	-22	-22
75	—	-10.5	-9	-9	-10	—	—	-13	-13
90	—	0	+2	0	+1.5	—	—	0	0

* U = upwind, D = downwind, and C = crosswind.

Table 10
Median Values of the Normalized Radar Cross Section σ_0 for
Directly Polarized Signals Measured at X, C, L, and P Bands

Feb. 20, 1969: Wind Velocity 29 knots; Wave Height 16.4 ft.

Depression Angle (degrees)	Wind Direction*	σ_0 (dB)							
		X_{VV}	X_{HH}	C_{VV}	C_{HH}	L_{VV}	L_{HH}	P_{VV}	P_{HH}
5	U	-35.5	-37.5	-34.5	-39.5	-40.5	-45	-41	-47
	D	-38.5	-43	-40	-44	-43	—	-43	—
	C	-37	-40.5	-39.5	-41.5	-44	-48.5	-42.5	—
10	U	-31.5	-35	-28.5	-38.5	-36	-48	-36	-46.5
	D	-33.5	-42.5	-31.5	-43.5	-34.5	-51	-36	-49
	C	-34.5	-39.5	-33.5	-41.5	-35.5	-48.5	-36	-49
20	U	-27	-33.5	-25	-35	-31	-41.5	-30	-47.5
	D	-29.5	-38.5	-28	-40	-29	-42.5	-28.5	-46.5
	C	-30	-38.5	-30	-40	-30.5	-43.5	-30.5	-45.5
30	U	-25.5	-30.5	-22	-32.5	-28	-37.5	-28.5	-37
	D	-27	-35.5	-23.5	-36.5	-26	-37.5	-28	-36.5
	C	-29	-35.5	-25.5	-35.5	-26.5	-36.5	-28	-37.5
45	U	-20.5	-24	-19	-27	-27	-33	-25.5	-31
	D	-23	-28.5	-21.5	-31	-25	-32	-24.5	-30.5
	C	-25.5	-29	-23.5	-30	-27	-34.5	-25.5	-32.5
60	U	-17.5	-18.5	-14.5	-19	-20.5	-22	-23	-25.5
	D	-18.5	-20	-16	-21	-19	-21.5	-22	-24.5
	C	-19.5	-20.5	-17.5	-21	-22	-24	-21	-24
75	—	-9.5	-10	-7	-9	—	—	-13	-15
90	—	-1	-1	+2	+1	—	—	+0.5	-2

* U = upwind, D = downwind, and C = crosswind.

DALEY, DAVIS, AND MILLS

Table 11
Median Values of the Normalized Radar Cross Section σ_0 for
Cross-Polarized Signals Measured at X, C, L, and P Bands

Feb. 6, 1969: Wind Velocity 40 knots; Wave Height 15 ft.

Depression Angle (degrees)	Wind Direction*	σ_0 (dB)							
		X_{VH}	X_{HV}	C_{VH}	C_{HV}	L_{VH}	L_{HV}	P_{VH}	P_{HV}
5	U	-44	-47.5	-46	Not	—	—	-43	-52
	D	-44	-48	-45.5	Record-	—	—	-43	—
	C	-41.5	-44	-44	ed	—	—	-45.5	—
10	U	-37.5	-40	-40.5	-39.5	—	—	-39	-46
	D	-39.5	-42.5	-43	-41	—	—	-37	-42.5
	C	-40	-42	-43	-42.5	—	—	-42	-48.5
20	U	-35.5	-37	-39	-36	-35	—	-37	-40
	D	-39.5	-41	-41	-39.5	-36	—	-38	-41
	C	-40.5	-41.5	-43	-41	-37.5	—	-41.5	-44
30	U	-33	-35	-36.5	-34	-34	-34	-37	-41
	D	-35	-36	-38.5	-35.5	-34.5	-35	-35	-40
	C	-34.5	-36	-38	-36	-34.5	-35	-37	-42.5
45	U	-29	-30.5	-33	-30	-30.5	-31	-34	-39
	D	-30	-32.5	-34	-31	-31.5	-32	-34	-39
	C	-31.5	-33	-35	-32.5	—	—	-37	-41.5
60	U	-28.5	-27.5	-29	-27	-27	-25.5	-32	-35.5
	D	-27.5	-28	-30.5	-27	-29	-27.5	-32	-36
	C	-28	-29	-32	-28.5	-30	-29.5	-34	-36.5

* U = upwind, D = downwind, and C = crosswind.

Table 12
Median Values of the Normalized Radar Cross Section σ_0 for
Cross-Polarized Signals Measured at X, C, L, and P Bands

Feb. 10, 1969: Wind Velocity 30-33 knots; Wave Height 11.5-13.1 ft.

Depression Angle (degrees)	Wind Direction*	σ_0 (dB)							
		X_{VH}	X_{HV}	C_{VH}	C_{HV}	L_{VH}	L_{HV}	P_{VH}	P_{HV}
5	U	-44	-47.5			-48	-48	-50.5	-55
	D	-44	-47			-53.5	—	-54.5	—
	C	-44.5	-48			-51.5	-52	-53.5	—
10	U	-41.5	-42			-43.5	-43.5	-45	-49
	D	-44.5	-44.5			-49.5	-48.5	-48.5	-51.5
	C	-44	-44.5			-48	-47.5	-49	-51.5
20	U	-38	-40.5			-39.5	-39	-43	-45.5
	D	-39.5	-42			-43	-42.5	-44.5	-48
	C	-40	-42.5	NOT RECORDED		-42.5	-41.5	-45.5	-47.5
30	U	-37.5	-38.5			-38.5	-37.5	-42.5	-44
	D	-37.5	-37			-41	-39	-42.5	-46
	C	-38	-38			-40.5	-39	-44.5	-45.5
45	U	-33.5	-34.5			-35	-33.5	-37.5	-41
	D	-33.5	-33.5			-37.5	-36	-39.5	-41
	C	-34.5	-34.5			-37	-36	-40	-42
60	U	-32	—			-30.5	-29.5	-37.5	-38.5
	D	-34.5	—			-32.5	-31	-38	-39.5
	C	-32.5	—			-33	-32	-37.5	-38.5

*U = upwind, D = downwind, and C = crosswind.

DALEY, DAVIS, AND MILLS

Table 13
Median Values of the Normalized Radar Cross Section σ_0 for
Cross-Polarized Signals Measured at X, C, L, and P Bands

Feb. 11, 1969: Wind Velocity 46-48 knots; Wave Height 21.3 ft.

Depression Angle (degrees)	Wind Direction*	σ_0 (dB)							
		X_{VH}	X_{HV}	C_{VH}	C_{HV}	L_{VH}	L_{HV}	P_{VH}	P_{HV}
5	U	-43	-47	-44.5	—	-46	—	-48.5	—
	D	-41.5	-46	-43.5	—	-49.5	—	-52	—
	C	-41.5	-46	-46.5	—	-49	—	-53	—
10	U	-42	-43.5	-42.5	-42	-40	-40.5	-43	-48.5
	D	-40	-41	-41	-40	-45.5	-45	-47	-51.5
	C	-40.5	-42	—	—	-46.5	-45.5	-49	-54.5
20	U	-36.5	-38	-38	-39	-37.5	-36.5	-44	-50.5
	D	-37.5	-38	-38.5	-40.5	-41	-38.5	-44.5	-49.5
	C	-38	-39	-40	-44	-43	-40	-46	-50
30	U	-35.5	-36	-35.5	-34.5	-35.5	-34.5	-39.5	-43.5
	D	-36.5	-37.5	-38.5	-37	-38	-36.5	-41	-44.5
	C	-35.5	-36.5	-38	-36.5	-39.5	-38	-43	-46.5
45	U	-31.5	-32	-34	-32.5	-34	-32.5	-40	-42.5
	D	-32	-32	-35.5	-34	-37	-34.5	-40	-43
	C	-32	-33.5	-36	-35.5	-37	-34.5	-42	-45
60	U	-30	-29.5	—	—	-29	—	—	-40
	D	-30.5	-29.5	—	—	-31	—	-38	-40
	C	-30	-29.5	—	—	-33	—	-39	-40.5
75	–	-28.5	—	—	—	—	—	—	—

* U = upwind, D = downwind, and C = crosswind.

Table 14
Median Values of the Normalized Radar Cross Section σ_0 for
Cross-Polarized Signals Measured at X, C, L, and P Bands

Feb. 13, 1969: Wind Velocity 35-39 knots; Wave Height 23 ft.

Depression Angle (degrees)	Wind Direction*	σ_0 (dB)							
		X_{VH}	X_{HV}	C_{VH}	C_{HV}	L_{VH}	L_{HV}	P_{VH}	P_{HV}
5	U	-43	-50	-42.5	—	-44	—	-48	--
	D	-43.5	-51	-43	—	-49	—	-50	—
	C	-44	-52	-43	—	-48.5	—	-50	—
10	U	-43	-46.5	-42.5	-43	-42.5	-44.5	-46	-50
	D	-42	-45.5	-43.5	-43.5	-45.5	-48	-48	-52
	C	-42	-45.5	-43	-44.5	-46	-48	-48.5	-52.5
20	U	-38.5	-42	-38	-40.5	-37	-39.5	-42	-46.5
	D	-39.5	-42.5	-39.5	-41.5	-40.5	-42.5	-43.5	-48
	C	-38.5	-41.5	-39.5	-43	-41.5	-44.5	-44.5	-48
30	U	-37	-40.5	-37	-36.5	-36	-36.5	-39.5	-42
	D	-37.5	-40	-37.5	-38	-39.5	-41	-41.5	-44
	C	-37	-39.5	-38.5	-40	-39	-40.5	-41.5	-44.5
45	U	-33	-36	-33	-32.5	-34	-35	-38.5	-41
	D	-34	-36	-34.5	-34	-36.5	-37	-40	-42
	C	-34	-36.5	-35.5	-37	-37.5	-38.5	-40.5	-43
60	U	-31.5	-32.5	—	—	—	—	-36.5	—
	D	-33.5	-34	—	—	—	—	-37	—
	C	-30.5	-32.5	—	—	—	—	-37.5	—

* U = upwind, D = downwind, and C = crosswind.

DALEY, DAVIS, AND MILLS

Table 15
Median Values of the Normalized Radar Cross Section σ_0 for
Cross-Polarized Signals Measured at X, C, L, and P Bands

Feb. 14, 1969: Wind Velocity 37-40 knots; Wave Height 23-26 ft.

| Depression Angle (degrees)	Wind Direction*	σ_0(dB)							
		X_{VH}	X_{HV}	C_{VH}	C_{HV}	L_{VH}	L_{HV}	P_{VH}	P_{HV}
5	U	-43	-49	-46	—	-47	—	-47.5	—
	D	-43.5	-49	-47	—	—	—	-49.5	—
	C	—	—	-45.5	—	—	—	—	—
10	U	-42	-45	-42.5	-42	-43.5	-44.5	-45	-50.5
	D	-42.5	-44.5	-43.5	-42.5	-49.5	-50.5	-48.5	-54.5
	C	—	—	-44.5	-46.5	-49	-49.5	-48.5	-53.5
20	U	-38.5	-41	-39.5	-39.5	-40	-40	-42.5	-47.5
	D	-38.5	-40.5	-39	-39	-43	-44	-44.5	-50
	C	-39	-42.5	-41.5	-42.5	-45	-45.5	-44.5	-50.5
30	U	-36.5	-38.5	-37	-35.5	-37	-37.5	-40	-43.5
	D	-37.5	-39.5	-39.5	-38	-40.5	-41	-41.5	-45.5
	C	-37	-39.5	-40.5	-41.5	-42	-43	-43.5	-47.5
45	U	-34.5	-36	-35	-33.5	-35.5	-37	-39.5	-42.5
	D	-34	-35	-36	-34	-37.5	-38	-40	-43.5
	C	-34	-36.5	-36.5	-37.5	-41	-41	-41	-45
60	U	-32	-32	—	—	-31	—	-37.5	-41
	D	-32	-32	—	—	-32	—	-38	-41
	C	-32	-33.5	—	—	-34	—	-38.5	-41.5

* U = upwind, D = downwind, and C = crosswind.

Table 16
Median Values of the Normalized Radar Cross Section σ_0 for
Cross-Polarized Signals Measured at X, C, L, and P Bands

Feb. 17, 1969: Wind Velocity 5 knots; Wave Height 3 ft.

Depression Angle (degrees)	Wind Direction*	σ_0(dB)							
		X_{VH}	X_{HV}	C_{VH}	C_{HV}	L_{VH}	L_{HV}	P_{VH}	P_{HV}
5	U	-49.5	-53	-51	—	—	—	-52	—
	D	-50	—	—	—	-51.5	—	-52	—
	C	-50	—	-51	—	-51.5	—	-52	—
10	U	-53.5	-57.5	-53.5	—	-51	-52.5	-50.5	-56
	D	-55.5	-60.5	-56.5	—	-50	-50.5	-50.5	-56
	C	-53.5	-57	-53.5	-55.5	-51.5	-52.5	-50.5	-56.5
20	U	-51.5	-58	-52	-51	-46	-46	-46	-48.5
	D	-49.5	-55.5	-52	-50.5	-44.5	-45.5	-45	-49.5
	C	-47	-54	-48.5	-46	-45.5	-46.5	-44.5	-48
30	U	-51.5	-54.5	-52	-49.5	-44	-44.5	-43	-46.5
	D	-50.5	-53.5	-51	-49	-42	-42.5	-43	-46
	C	-48.5	-50.5	-48	-46.5	-42.5	-43	-42.5	-45.5
45	U	-50	-51	—	—	-41	-40.5	-41.5	-43.5
	D	-48	-50.5	—	—	-39.5	-38.5	-42	-44
	C	-48.5	-49.5	—	—	-41	-41.5	-41	-43
60	U	—	—	—	—	—	—	-38.5	-41
	D	—	—	—	—	—	—	-38	-41
	C	—	—	—	—	—	—	-37.5	-40

* U = upwind, D = downwind, and C = crosswind.

DALEY, DAVIS, AND MILLS

Table 17
Median Values of the Normalized Radar Cross Section σ_0 for
Cross-Polarized Signals Measured at X, C, L, and P Bands

Feb. 18, 1969: Wind Velocity 22 knots; Wave Height 9.8 ft.

Depression Angle (degrees)	Wind Direction*	σ_0 (dB)							
		X_{VH}	X_{HV}	C_{VH}	C_{HV}	L_{VH}	L_{HV}	P_{VH}	P_{HV}
5	U	-45	-50.5	-43	—	-48.5	—	-48	—
	D	-46.5	-53	-43.5	—	-49	—	-48.5	—
	C	-45.5	-50.5	-43.5	—	-47.5	—	-47.5	—
10	U	-44.5	-49.5	-45	-47.5	-46	-45.5	-46	-52.5
	D	-45.5	-50	-45.5	-47.5	-49	-49.5	-48.5	-55
	C	-46	-51.5	-47.5	-53	-49	-49.5	-47.5	-53.5
20	U	-42	-45	-41	-44	-42	-42	-42.5	-48
	D	-42	-45.5	-41.5	-44	-43.5	-42	-42.5	-48
	C	-44.5	-47	-44	-47.5	-44.5	-44.5	-42	-47
30	U	-40	-42.5	-40.5	-41	-39	-38	-39.5	-44
	D	-41	-43	-41	-43	-41	-40.5	-40.5	-46
	C	-42.5	-45.5	-43.5	-47	-43	-42.5	-40.5	-45.5
45	U	-36.5	-38	—	—	-37	-35.5	-38.5	-43
	D	-36.5	-37.5	—	—	-40	-39	-38.5	-43.5
	C	-39	-41.5	—	—	-40	-39	-39.5	-44.5
60	U	-36	-36.5	—	—	—	—	-36	-40.5
	D	-34	-35.5	—	—	—	—	-36	-40.5
	C	-39.5	-39.5	—	—	—	—	-36.5	-41

* U = upwind, D = downwind, and C = crosswind.

Table 18
Median Values of the Normalized Radar Cross Section σ_0 for
Cross-Polarized Signals Measured at X, C, L, and P Bands

Feb. 20, 1969: Wind Velocity 29 knots; Wave Height 16.4 ft.

Depression Angle (degrees)	Wind Direction*	σ_0 (dB)							
		X_{VH}	X_{HV}	C_{VH}	C_{HV}	L_{VH}	L_{HV}	P_{VH}	P_{HV}
5	U	-44	-47.5	-42	—	-47	—	-47	—
	D	-46	-51	-43	—	-48.5	—	-48	—
	C	-44.5	-47.5	-43.5	—	—	—	-47.5	—
10	U	-42.5	-43.5	-41	-43	-48.5	-50	-45.5	-51
	D	-46	-46.5	-44.5	-46	-48	-48.5	-46	-51
	C	-45.5	-47	-44	-47	-47.5	-48.5	-46.5	-51.5
20	U	-39	-40	-38	-39	-42.5	-45	-42	-46
	D	-42	-43.5	-40.5	-40.5	-42	-41.5	-42	-45
	C	-43	-43.5	-41	-43	-43.5	-45	-42	-45
30	U	-38	-39	-36.5	-36	-41	-41.5	-40	-43.5
	D	-40	-41	-38	-38	-39.5	-39	-40.5	-44
	C	-40	-40.5	-38	-38.5	-39	-39.5	-40.5	-43.5
45	U	-36	-35	-34.5	-33.5	-41	-40.5	-40	-42.5
	D	-38	-37.5	-36	-36	-38.5	-38	-38.5	-41.5
	C	-37.5	-37	-36.5	-37	-41.5	-42	-40	-43
60	U	-35	-33.5	—	—	—	—	-38.5	-40.5
	D	-35	-34	—	—	—	—	-37.5	-39.5
	C	-34.5	-33.5	—	—	—	—	-37	-39.5

* U = upwind, D = downwind, and C = crosswind.
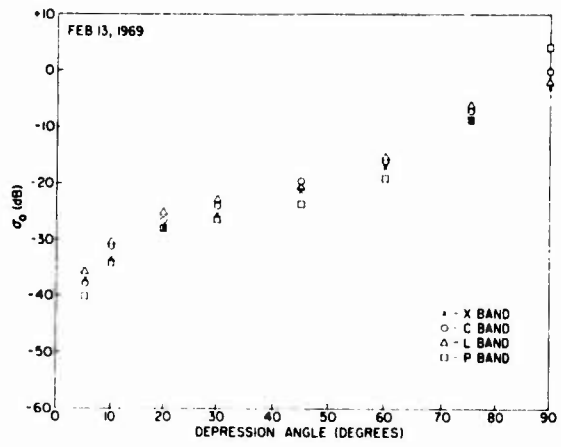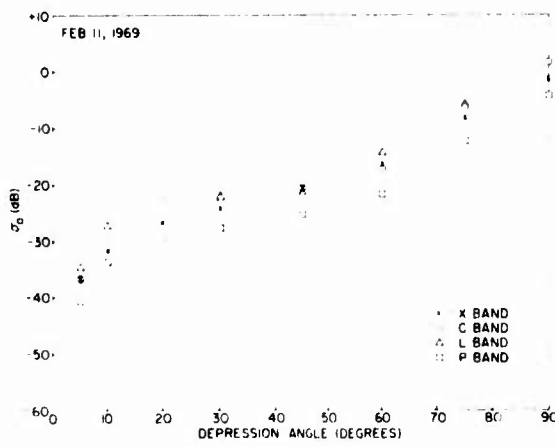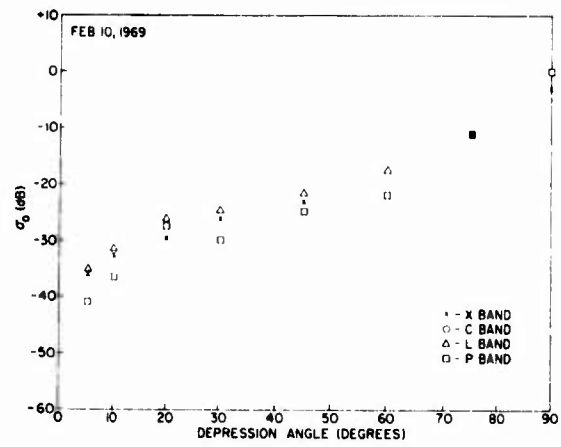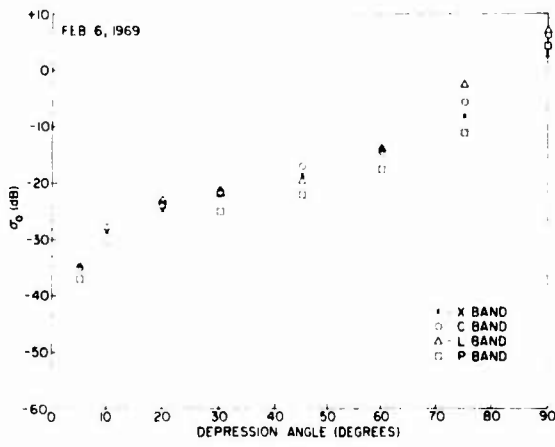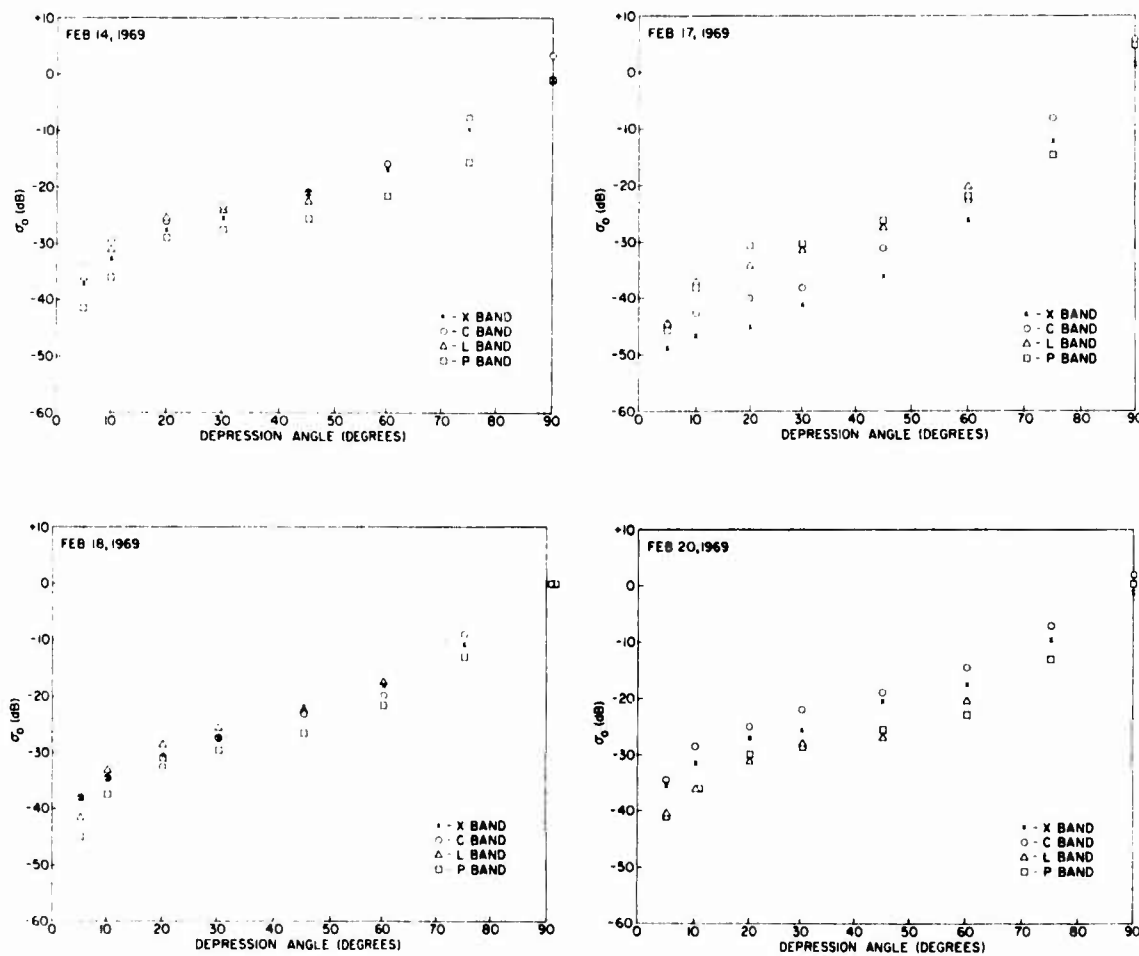
Fig. 6 - Normalized radar cross section σ_0 of the ocean vs depresion angle for direct, vertically polarized (VV), radar signals. Data are for upwind conditions on all dates.
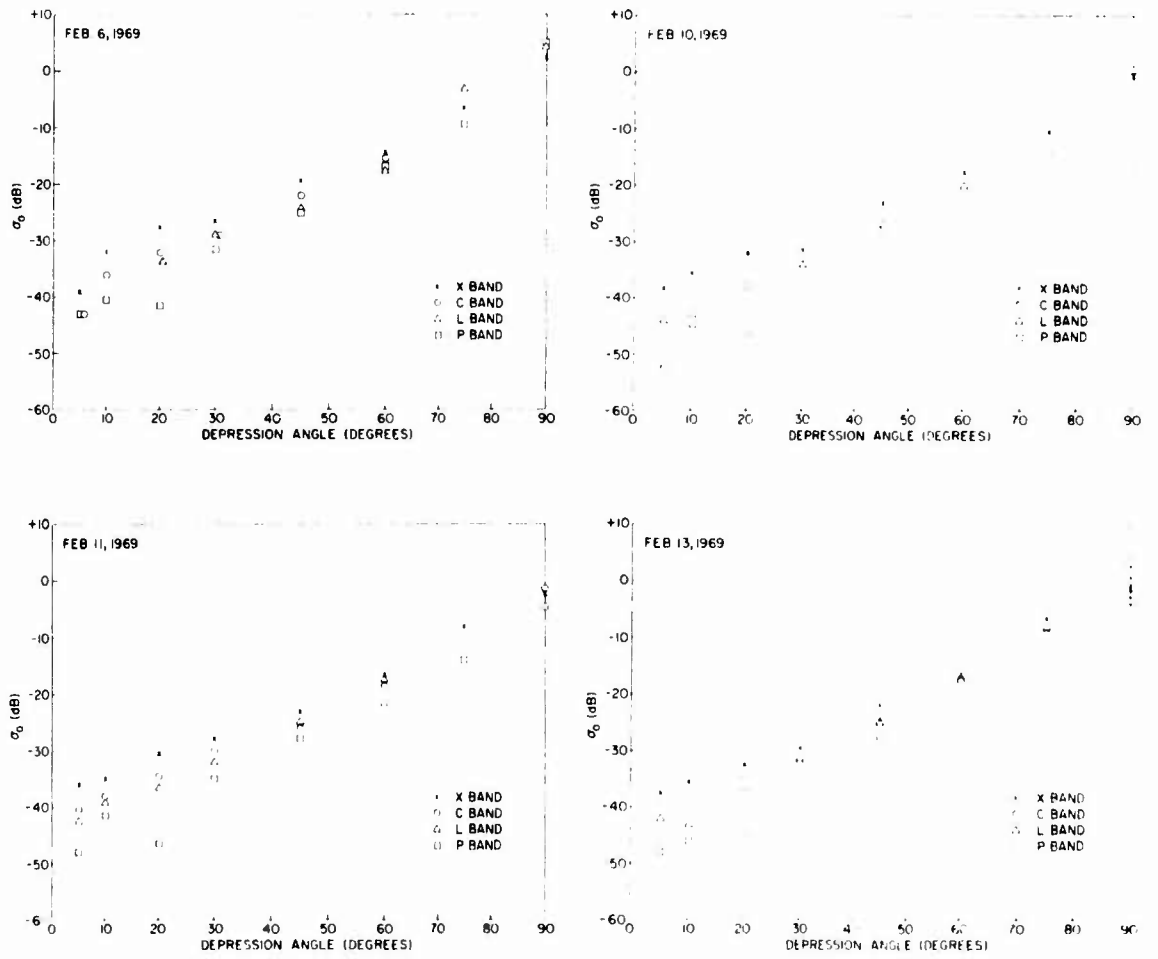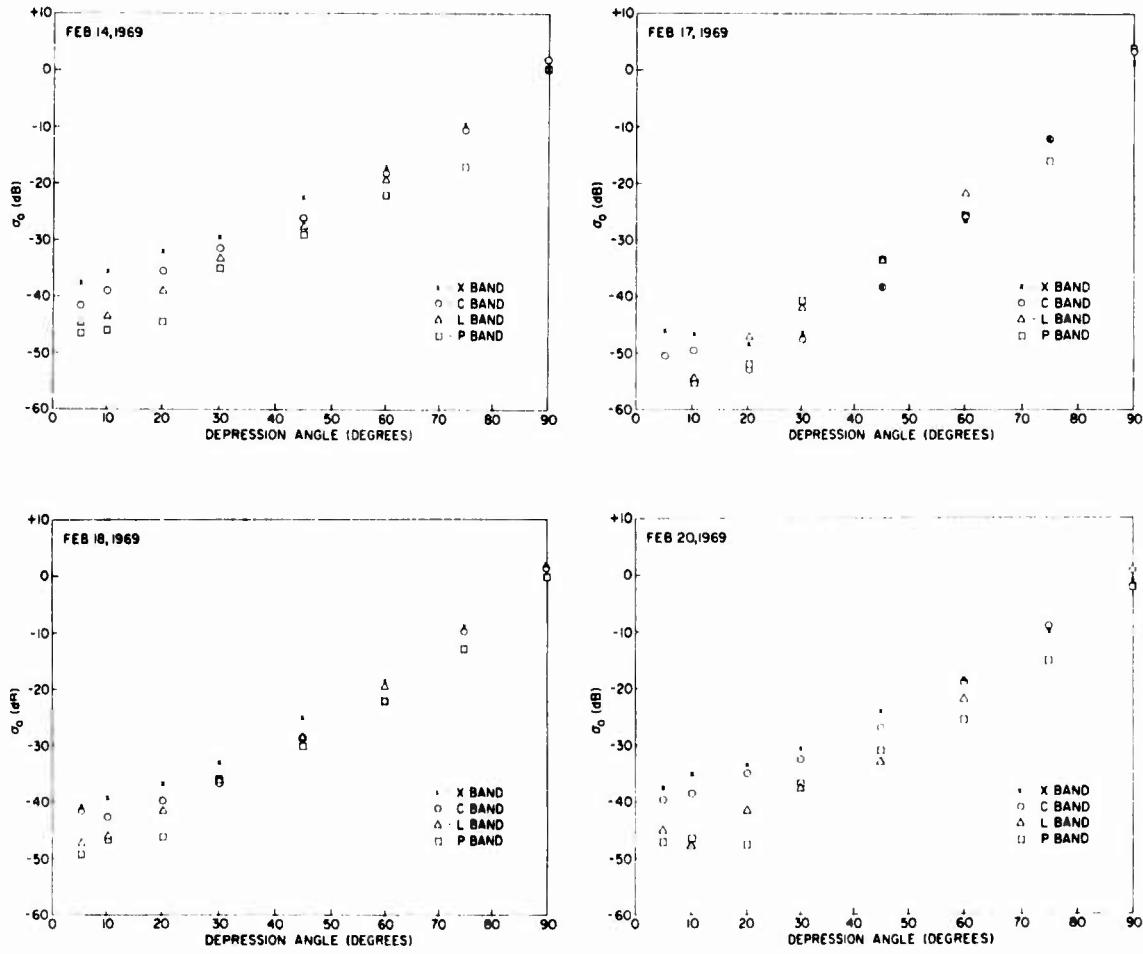
Fig. 7 - Normalized radar cross section σ_0 of the ocean vs depression angle for direct, horizontally polarized (HH), radar signals. Data are for upwind conditions on all dates.

DALEY, DAVIS, AND MILLS
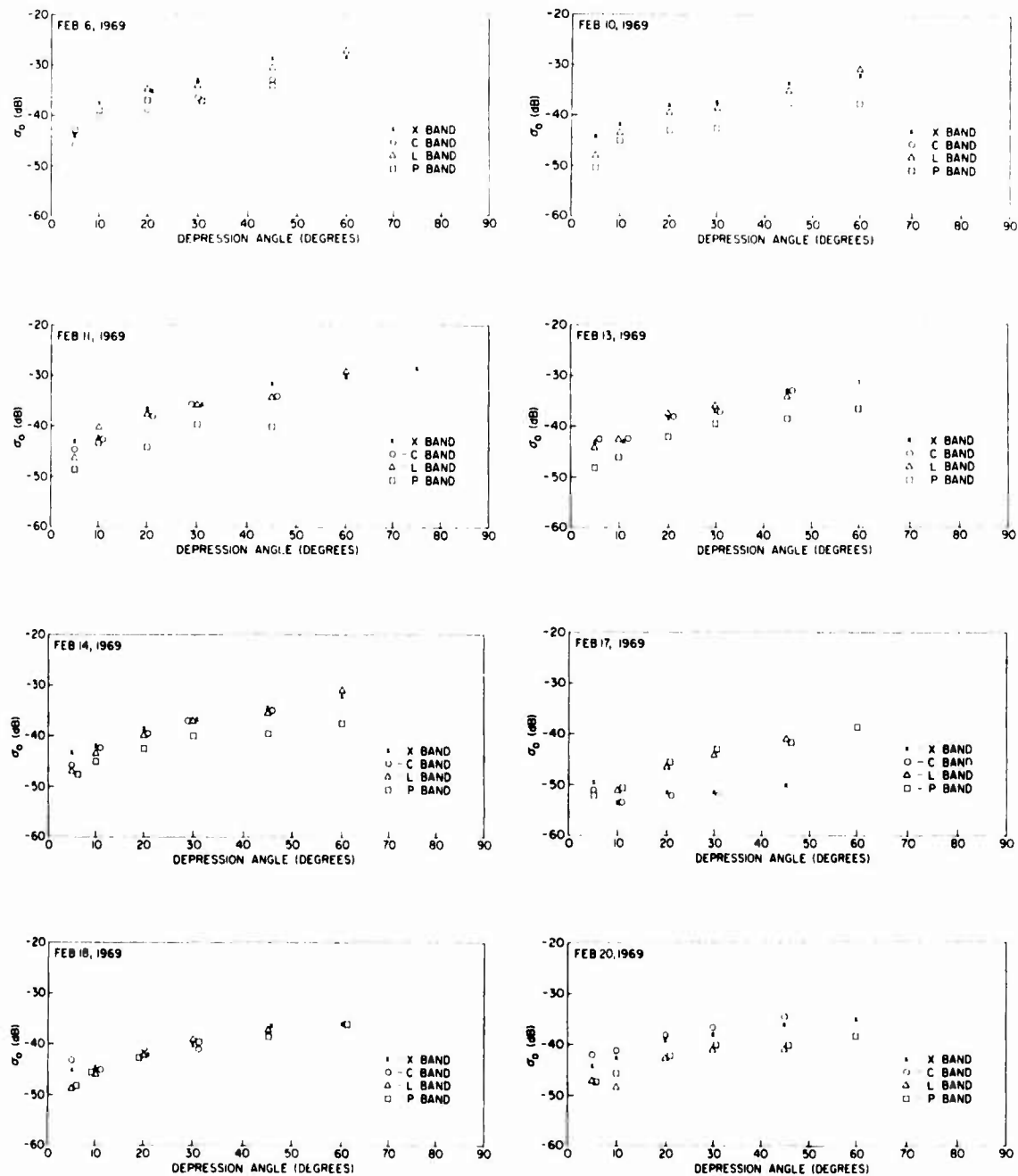
Fig. 8 – Normalized radar cross section σ_0 of the ocean vs depression angle for cross-polarized (VH) radar signals. Data are for upwind conditions on all dates.

As evidenced by the curves, σ_0 is wavelength dependent for *HH* polarization (Fig. 7), whereas no clear trend is present in the *VV* case (Fig. 6), except for the relatively calm sea on February 17, 1969. Replotting the data of February 14, 1969, in Fig. 9a shows a definite trend for the HH polarization on nonvertical incidence from X band to P band, which can be approximated by $\sigma_0 \sim \lambda^{-1/2}$ or $\sigma_0 \sim \lambda^{-1}$. No such trend is observable for the vertical polarization case (Fig. 9b) from X band to L band, although P band decreases sharply. The cross-polarized return tends to be less dependent on wavelength for the high seas (Fig. 8), but it should be noted that the P band is consistently lower than the other frequencies.

The relationship of the normalized cross section σ_0 to polarization is conveniently expressed by the direct-polarization ratio $(\sigma_0)_{VV}/(\sigma_0)_{HH}$ simply calculated in decibels. Figure 10 shows this parameter as a function of angle for each radar wavelength and sea condition. It is apparent that even on the roughest days, the polarization ratio is significant for all wavelengths in the moderate angle region, and has a tendency to decrease as grazing is approached. The wavelength dependence as observed previously is also reflected in the direct-polarization ratio. The ratio increases with wavelength, and the magnitudes here are comparable to those measured at Puerto Rico in 1965 (2).

DEPENDENCE OF σ_0 ON SURFACE PARAMETERS

The data discussed above have been solely for the upwind case. This has been necessary due to the fact that significant upwind-to-downwind and upwind-to-crosswind differences were consistently observed as is evident in the data tables. The ratios $(\sigma_0)_{upwind} (\sigma_0)_{downwind}$ and $(\sigma_0)_{upwind}/(\sigma_0)_{crosswind}$ were investigated as functions of polarization, depression angle, and radar wavelength. Although absolute magnitudes varied from day to day, the general behavior observed at the sea states encountered is exemplified in the data from February 11, 1969 (Fig. 11). The most unexpected feature is the consistently high (≈ 5 dB) upwind-to-crosswind ratio, even for the long radar wavelengths. If one equates increased surface roughness with increased randomness, then one does not expect a relationship between clutter and wind direction. However, visual observation, as well as aerial photographs (Figs. 12a and b), showed a highly directional sea. The "streaky" appearance of the surface in Fig. 12a was observed to be due to windblown spray, so that different scatters, present in the upwind direction, apparently enhance the clutter.

To estimate the effect of increasing sea states on the normalized RCS σ_0, it is necessary to select a surface parameter which will reflect increasing roughness. As a first approximation, the median wind velocity was chosen, and plots of σ_0 versus median wind were made for all signal components measured for depression angles from 5 to 75°, including previous 4FR data taken at Puerto Rico in 1965 (2). A set of typical curves are given in Fig. 13 for upwind conditions and a depression angle of 30°; the plots demonstrate a common result, namely, that σ_0 approaches a saturation value as surface roughness increases. The data further indicate that the relationship of σ_0 to wind velocity is a function of radar wavelength and, to a lesser extent, polarization. Wind is not a descriptor of clutter except at the shorter wavelengths (X and C bands). In those cases σ_0 increases with wind velocity up to speeds of about 10-15 knots, where the value of σ_0 is seen to increase at a slower rate or not at all. As is evident from the figures, there is little or no increase in clutter with increasing wind velocity on the longer wavelengths, and for all wavelengths the value of σ_0 approaches an upper limit. This limit has been calculated for a full developed sea, whose wave spectrum has been approximated by the Phillips-Burling equilibrium spectrum (see the Appendix). The predicted value is seen to provide an upper bound to σ_0 for the roughest seas encountered to date (6).

DALEY, DAVIS, AND MILLS
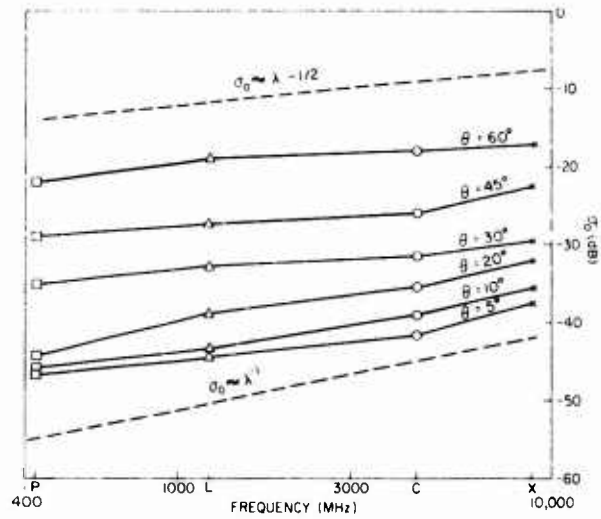
(a)
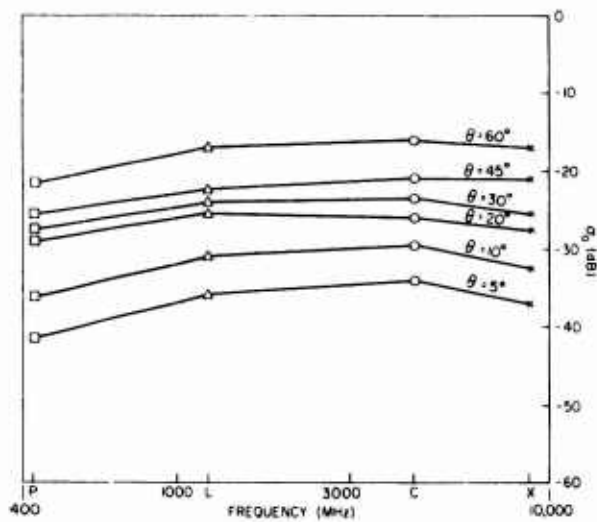
(b)

Fig. 9 - Normalized radar cross section σ_0 of the ocean vs transmitted radar frequency for (a) *HH* polarization and (b) *VV* polarization. Data are for upwind conditions on Feb. 14, 1969.
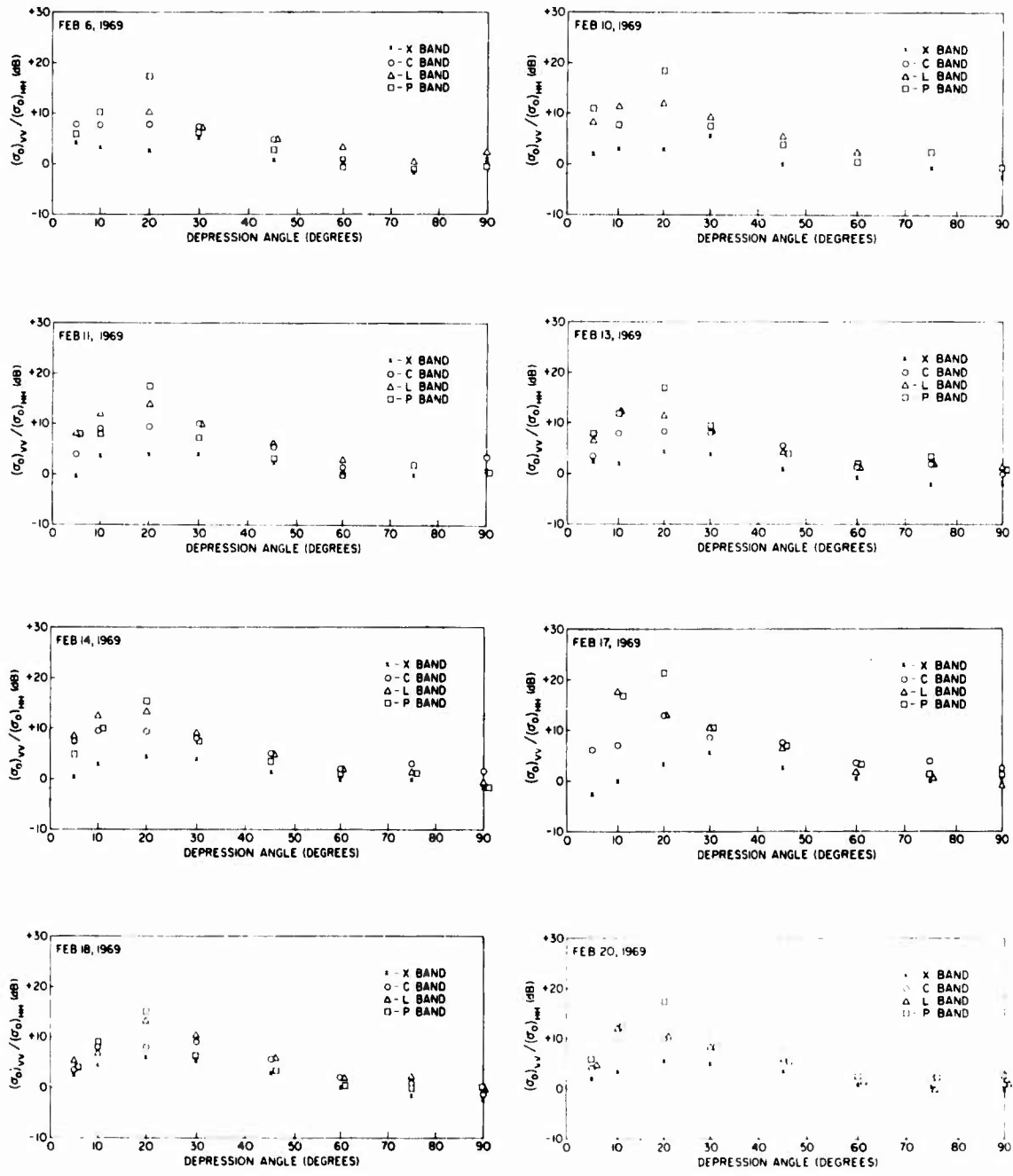
Fig. 10 - Ratio of direct vertically polarized (VV) to direct horizontally polarized (HH) radar signals vs depression angle. These plots of $(\sigma_0)_{VV}/(\sigma_0)_{HH}$ conveniently display the effects of signal wavelength, sea condition, and depression angle on the direct-polarized returns. Data are for upwind conditions on all dates.
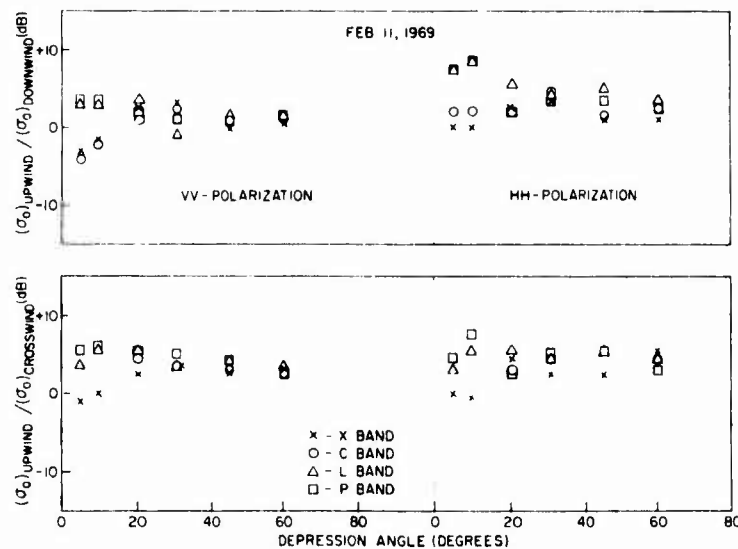
Fig. 11 - Upwind-to-downwind and upwind-
to-crosswind radar cross-section ratios
vs depression angle. This plot also il-
lustrates the effects of signal wavelength
and polarization direction on the cross
section. Data are for a 46-48 knot wind
on Feb. 11, 1969.

The high-sea-state data discussed above have been combined with work on previous
4FR data (chiefly from Puerto Rico in 1965) in a compact format for use by radar sys-
tems designers (7). Also, a recent review (8) provides a summation and evaluation of
clutter work done prior to the high-sea-state program.

SYSTEM LIMITATIONS

The two basic uncertainties in the calibration of the 4FR measurement system are
the receiver stability and the measurement of the sphere. The receiver stability is
monitored by inserting a known signal in the r-f line and recording it periodically through
the data collecting period. This signal serves to quantize receiver drift and any changes
in sensitivity through the data taking period. The sphere measurement possesses an
uncertainty due to the variation of illumination of the sphere signal in the center of the
beam. This uncertainty is minimized by repeating the sphere measurements on each
radar frequency and then calibrating on the maximum value of the sphere return. The
statistical scatter of the sphere return, about a (range) $^{-4}$ slope, is the limit of error of
the sphere measurement. Both of the above errors have been combined (worst case)
and listed in Table 19. The limits apply to absolute values of σ_0 for each signal com-
ponent, with exceptions noted below.

The exceptions to the above error analysis include measurements at depression
angles of 90 (normal incidence) and measurements of the cross-polarized components.
The measurement at 90° has inherent in it a problem of range gating at the center of the
antenna beam, which is not present at other angles. The specular nature of the return
at 90°, plus vertical platform motion, causes difficulty in continuous range gating at the
center of the clutter pile. For this reason, although values are given at 90°, we have

WIND

(a)
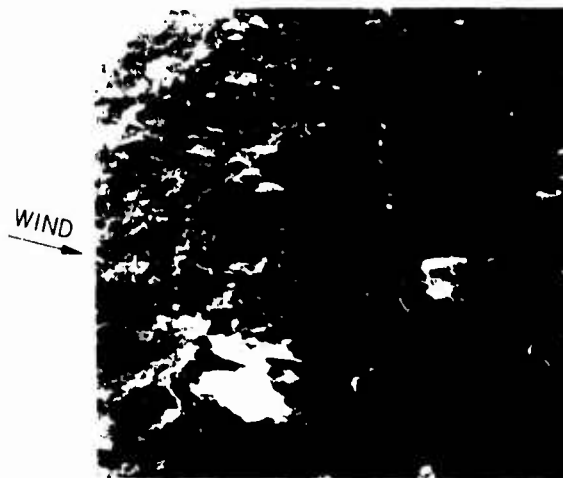
WIND

(b)

Fig. 12 - Aerial photographs of the ocean surface
on Feb. 11, 1969.   A 46-48 knot wind condition
prevailed.

avoided drawing general conclusions for this particular case. The cross-polarized re-
turn is subject to contamination due to system crosstalk, mostly at the antenna and
receiver.   These data are calibrated by the appropriate direct-polarized sphere meas-
urement, e.g., X_{VH} data are calibrated by the X_{HH} sphere, X_{HV} data are calibrated by the
X_{VV} sphere.   This procedure assumes no major differences between vertical and hori-
zontal transmission. This is generally true, and in that case the cross-polarized values
of $_0$ would have the same limits of error as the appropriate direct-polarized value.
These limits of error account for the spread between VH and HV values in most cases,
with one exception: On P band, the VH aspect is consistently higher than the HV, by
amounts beyond those expected due to the above-mentioned errors. In this case, the
best estimate of cro -polarized RCS is the median value of VH and HV.
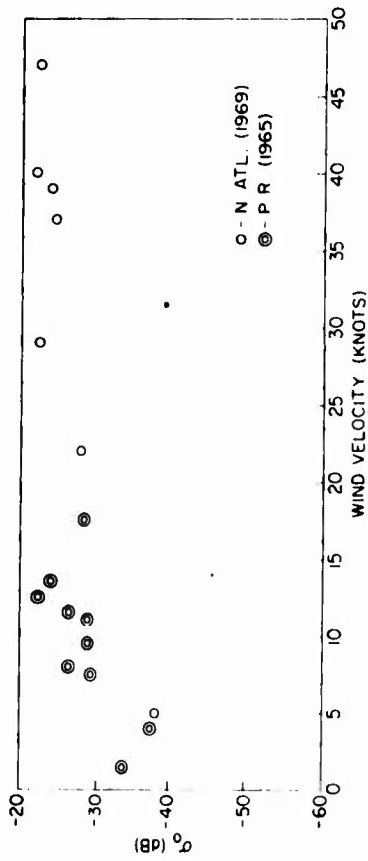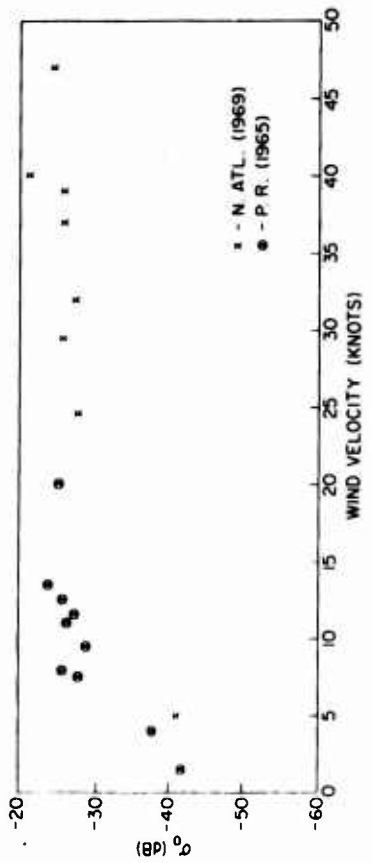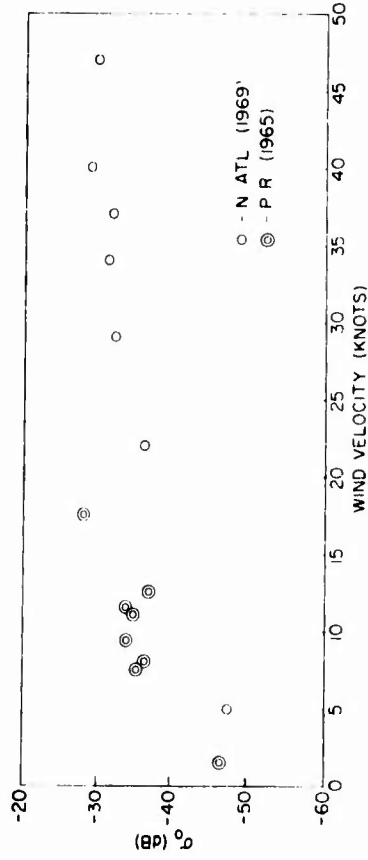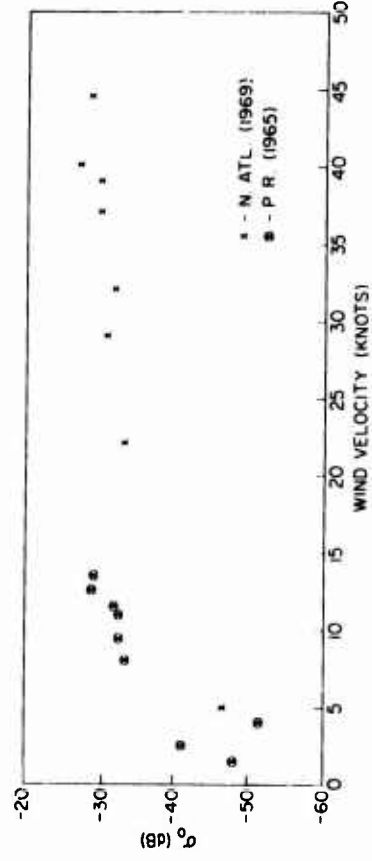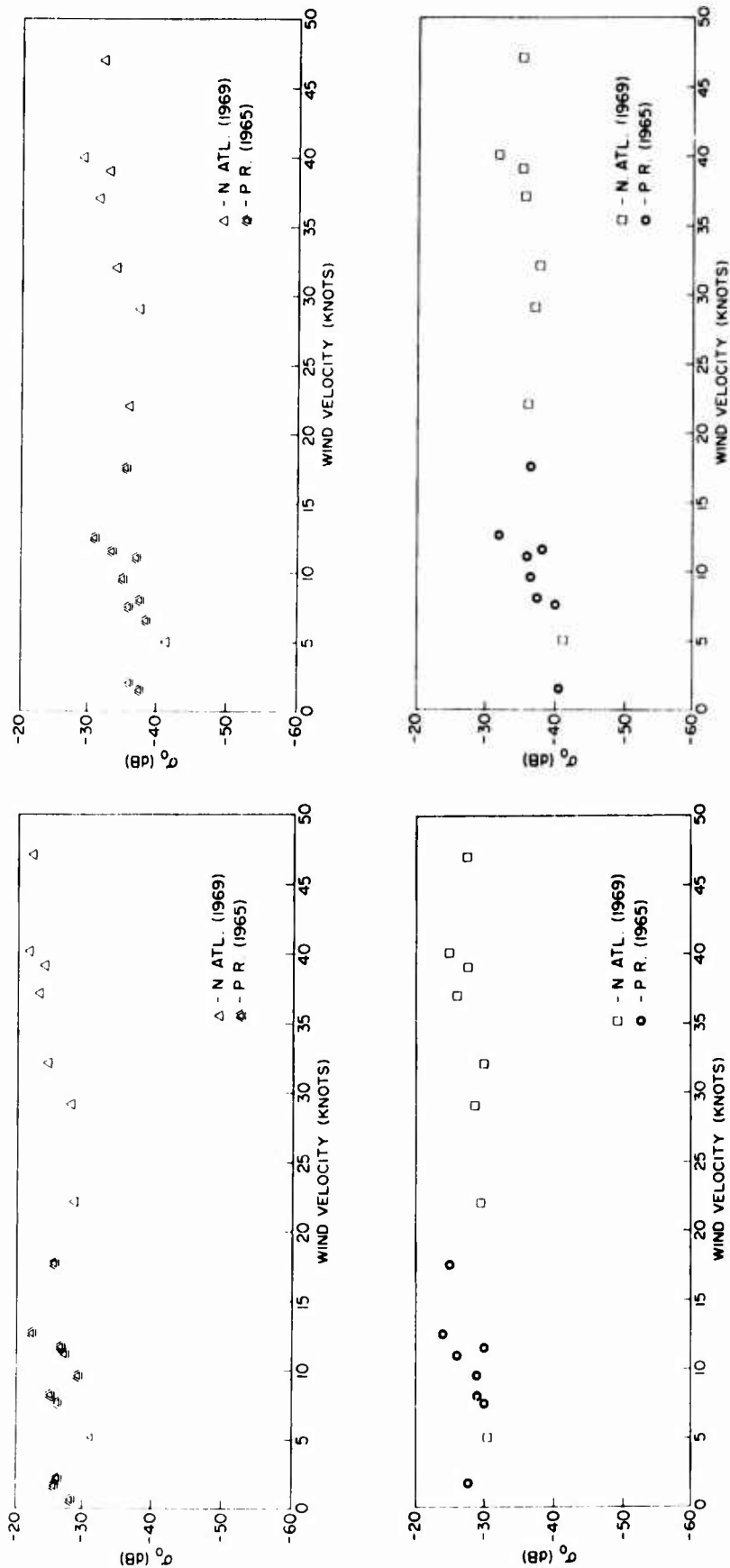
Fig. 13 – Normalized radar cross section σ_0 of the ocean vs wind velocity for direct vertically polarized (VV) and horizontally polarized (HH) radar signals. Data are for upward conditions and a depression angle of 30° in all cases. By combining the Puerto Rico (P. R.) and North Atlantic (N. Atl.) data it can be seen that σ_0 approaches a saturation value as the sea surface roughness increases.

DALEY, DAVIS, AND MILLS

Table 19
Limits of Error (Worst Case) in Absolute Measurements of σ_o

Date	Error (dB)							
(1969)	X_V	X_H	C_V	C_H	L_V	L_H	P_V	P_H
Feb. 6	±2.5	±2.5	±2.5	±1	±2	±3	±2	±2
Feb. 10	2	2	—	—	1.5	2	4	2
Feb. 11	1.5	1	2	1	3	3.5	1	1
Feb. 13	1.5	1	2	1.5	3.5	2.5	1	2
Feb. 14	1.5	1	1.5	1.5	1.5	1	1	2.5
Feb. 17	1	1	2	1.5	2.5	3	1.5	1
Feb. 18	2	1.5	1	1	2	1.5	1	1
Feb. 20	1	1	1.5	1	1.5	1.5	1.5	2

CONCLUSIONS

The processing and analysis of radar backscatter data, recorded in the North Atlantic in February 1969, have been completed at NRL. Radar returns were collected on four radar frequencies in both linear (VV or HH) and cross (VH or HV) polarizations, and the data were processed to obtain the normalized radar cross section (RCS) σ_0 of the sea surface as a function of radar and surface parameters for the high sea states encountered. The study of the behavior of the median value of σ_o as a function of the radar parameters and sea conditions resulted in the following conclusions at high sea state (characterized by winds of 20-50 knots and wave heights of 10-26 ft):

1. The angular variation of $(\sigma_0)_{VV}$ and $(\sigma_0)_{HH}$ conforms to previous results and is not significantly different as the sea state increases.

2. The value of σ_0 is independent of radar signal wavelength for vertical polarization, but maintains an inverse wavelength dependence $(\sigma_0 \sim \lambda^{-1}$ $^2 \sim \lambda^{-1})$ for horizontal polarization.

3. The cross-polarization return is less dependent on wavelength in the moderate depression angle region ($20°$-$60°$) from X band to L band, with P-band results being considerably lower.

4. The direct-polarization ratio $(\sigma_0)_{VV}$ $(\sigma_0)_{HH}$ remains significant for all wavelengths as the sea roughness increases, and is a function of wavelength.

5. The value of σ_0 is sensitive to wind direction, with consistently higher values observed in the upwind direction for all wavelengths and for both direct polarizations.

6. The value of σ_0 does not increase significantly with wind velocity in the region from 20 to 50 knots encountered in the North Atlantic.

7. All 4FR sea clutter data taken to date indicate that σ_o approaches a maximum or "saturation" value with increasing sea surface roughness.

In addition to the basic data contained in this report, the high-sea-state measurement program has provided a comprehensive data bank of pulse-to-pulse returns which may be analyzed to develop statistical models of the sea clutter process. Finally, as a continuation of these studies, in January 1970 a measurement program, investigating sea return, was conducted in the vicinity of Argus Island near Bermuda which has provided considerable additional data documenting the variation of cross section with wind in the critical wind velocity region near 10 knots. A further study has been made off the east coast of the United States to investigate the behavior of the RCS at P and L bands in the shallow grazing angle region below $5°$ which hopefully will provide insight into the effect of large swell structure on the clutter cross section at these angles. As a result of these studies, it is hoped that many of the difficulties inherent in the design and specification of the characteristics of ocean surveillance systems, which are related to the clutter background, will be resolved and that the performance of these systems in a clutter-limited environment will become increasingly predictable.

REFERENCES

1. Kerr, D.E , ed., "Propagation of Short Radio Waves," MIT Rad. Lab. Series, New York:McGraw-Hill, Vol 13, p. 481, 1951.

2. Daley, J.C., Ransone, J.T., Jr., Burkett, J.A., and Duncan, J.R., "Sea-Clutter Measurements on Four Frequencies," NRL Report 6806, Nov. 1968.

3. Guinard, N.W , "The NRL Four-Frequency Radar System," Report of NRL Progress, pp. 1-10, May 1969.

4. Wright, J W., "A New Model for Sea Clutter," IEEE Trans., AP 16 (No. 2): 217-223 (1968).

5. Valenzuela, G.R., "Depolarization of EM Waves by Slightly Rough Surfaces," IEEE Trans., AP-15 (No. 4): 552-557 (1967).

6. Guinard, N.W., and Daley, J.C., "An Experimental Study of a Sea Clutter Model," Proc. IEEE 58: 543-550 (1970).

7. Daley, J.C., Davis, W.T., and Mills, N.R., "Sea Return Standard," NRL Memorandum Report 2066, Nov. 21, 1969.

8. Skolnik, M.I., "A Review of Radar Sea Echo," NRL Memorandum Report 2025, July 1969.

Appendix

DERIVATION OF UPPER LIMIT FOR σ_0

In order to arrive at an expression for the normalized radar cross section σ_0 at saturation, which will provide a theoretical upper limit to the value of the radar cross section (RCS), the conditions under which a surface can be considered slightly rough in the sense of Rice (A1) must be stated. These are

$$\left| \beta f(x, y) \right| << 1$$

for the heights and

(A1)

$$\left| \frac{\partial f(x, y)}{\partial y} \right| << 1 \quad \text{and} \quad \left| \frac{\partial f(x, y)}{\partial x} \right| << 1$$

for the slopes of the surface, respectively. With this specification, several authors (4, 5, A2, and A3) have determined that the RCS of the slightly rough surface for the directly polarized returns (linear) are, to the first order, given by

and

$$\left(\sigma_0 \right)_{HH} \approx 4 \pi \beta^4 \sin^4 \theta \, \alpha_{HH} \, W(K_x K_y)$$

$$\left(\sigma_0 \right)_{VV} \approx 4 \pi \beta^4 \sin^4 \theta \, \alpha_{VV} \, W(K_x, K_y)$$

(A2)

where β is the wave number of the incident radar energy, θ is the depression angle, K_x and K_y are the wave numbers in the x and y direction on the infinite surface, and W is the two-dimensional energy density spectrum of the surface height variations. The α terms are given by

$$\alpha_{HH} \approx \left| \frac{(\epsilon - 1)}{\left(\sin \theta + \sqrt{\epsilon - \cos^2 \theta} \right)^2} \right|^2$$

and

(A3)

$$\alpha_{VV} \approx \left| \frac{(\epsilon - 1) \left(\epsilon (\cos^2 \theta + 1) - \cos^2 \theta \right)}{\left(\epsilon \sin \theta + \sqrt{\epsilon - \cos^2 \theta} \right)^2} \right|^2$$

where ϵ is the complex dielectric constant.

To proceed further, following Wright (A4) the spectrum of the surface height variations must be evaluated. As previously noted, Phillips (A5) had investigated the growth mechanisms of water waves and had concluded that an upper limit exists for the height of a wave of fixed length whether in the gravity or capillary range. In the former, the height is limited by the extraction of energy in surface detachment or breaking, while in the latter it is limited by the development of sharp troughs and energy loss through the release of bubbles. Using a dimensional argument, Phillips found that in these portions

40

of the ocean wave spectrum, i.e., in the equilibrium range, the spectrum is of the
form

$$W(K) = BK^{-4}$$

$$(A4)$$

where $K = \sqrt{K_x^2 + K_y^2}$ and the constant B is averaged over the entire surface. There is
some uncertainty in the value of the constant; however, using data from several sources,
Phillips has determined that the value of B should be 6×10^{-3} for the equilibrium range
spectrum for gravity waves and 1.5×10^{-2} for the capillary wave spectrum. Substituting
Eq. A4 into A2 and evaluating at wave numbers satisfying the Bragg scattering condition,
i.e.,

$$K_x = 2 \cos \quad \text{and} \quad K_y = 0,$$

$$(A5)$$

the limiting form of the cross section for angles away from the surface normal is found
to be

$$\left(_0 \right)_{HH} = (1.5) \times 10^{-3} \, _{HH} \tan^4 .$$

and

$$(A6)$$

$$\left(_0 \right)_{VV} = (1.5) \times 10^{-3} \, _{VV} \tan^4 $$

where $0 \leq \quad /2$, B has been set equal to 6×10^{-3}, and the 's are as defined previously.

Figures A1 through A4 relate the predicted values of $_0$, calculated from Eq. A6, to
the North Atlantic data. RCS values are shown for various wind velocities, with the
February date on which the data were obtained given in parentheses to the right of the
wind velocity.

One striking characteristic of these relationships is that for vertical polarization
they yield the accepted shape for the cross section versus grazing angle variation (- -
curve) and also the observed polarization dependence (for flat surfaces) without invoking
the interference phenomenon which was previously thought to be responsible for these
effects. Another is that, except for the variation of the dielectric constant, the cross
section at saturation is independent of the transmitted radar wavelength.
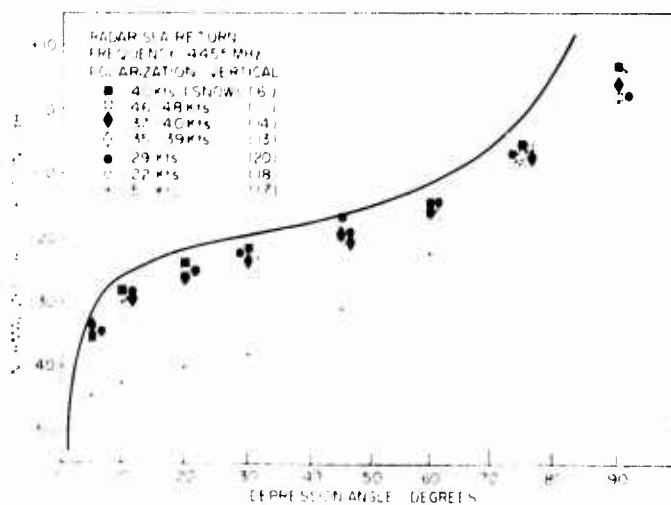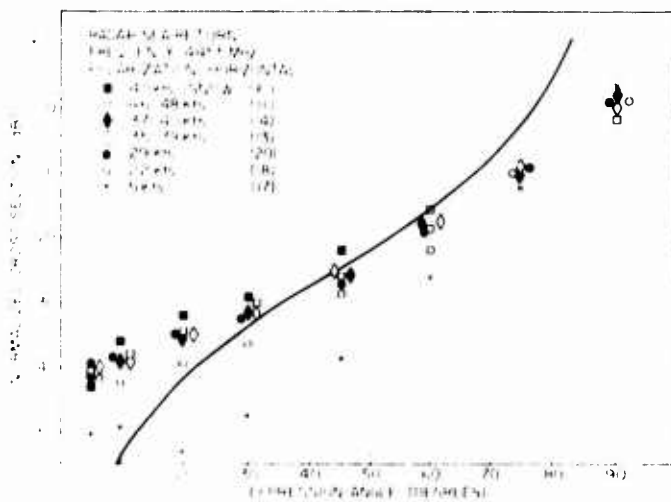
DALEY, DAVIS, AND MILLS
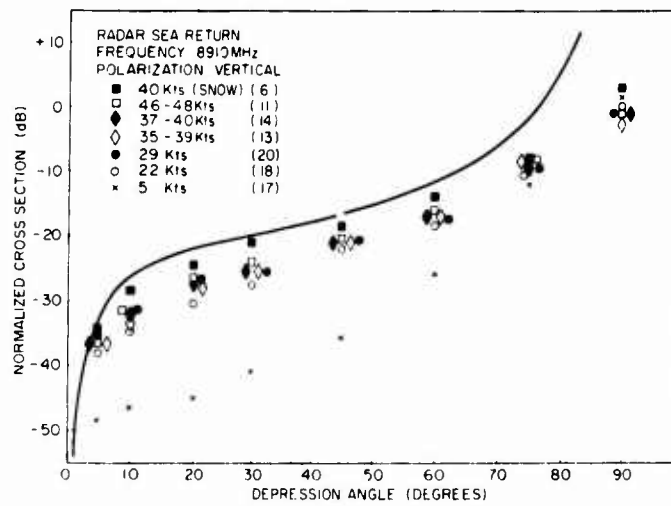
(a)
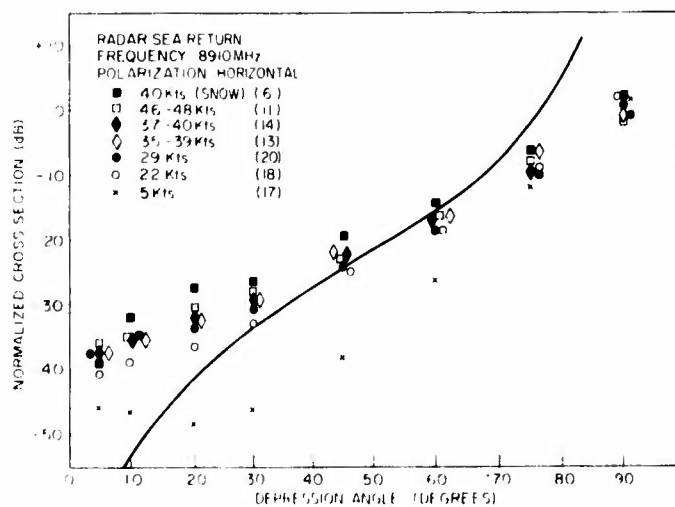
(b)

Fig. A1 - Normalized radar cross section σ_0 of the ocean vs depression angle for (a) direct, vertically polarized, and (b) direct, horizontally polarized radar signals at X-band frequency (8910 MHz). All data are for upwind conditions.
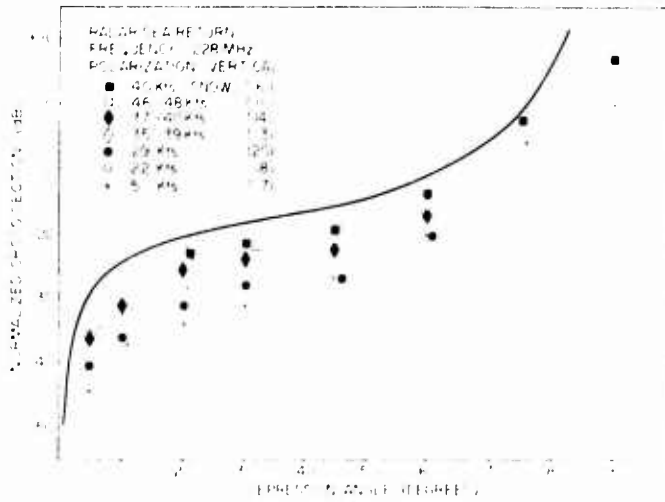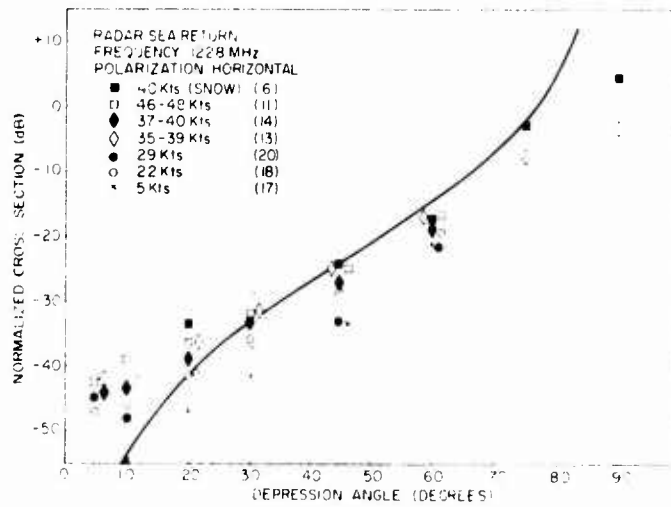
(a)

(b)

Fig. A2 - Normalized radar cross section σ_0 of the ocean vs depression angle for (a) direct, vertically polarized, and (b) direct, horizontally polarized radar signals at C-band frequency (4455 MHz). All data are for upwind conditions.
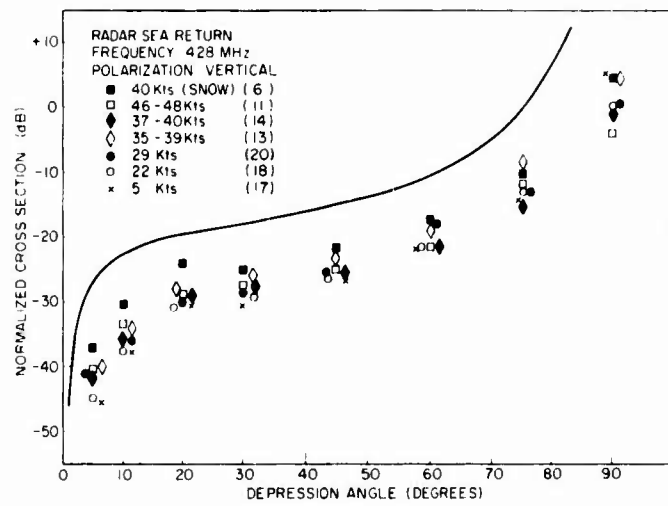
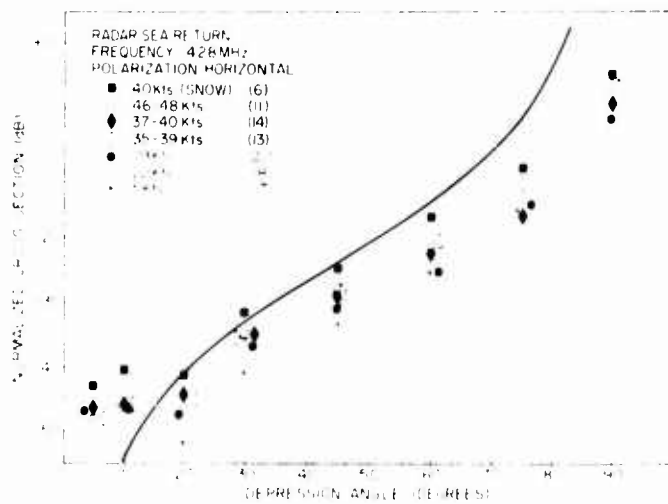DALEY, DAVIS, AND MILIS

(a)

(b)

Fig. A3 - Normalized radar cross section σ_0 of the ocean
vs depression angle for (a) direct, vertically polarized,
and (b) direct, horizontally, polarized radar signals at
L-band frequency (1228 MHz). All data are for upwind
conditions.

(a)

(b)

Fig. A4 - Normalized radar cross section $_0$ of the ocean vs depression angle for (a) direct, vertically polarized, and (b) direct, horizontally polarized radar signals at P-band frequency (428 MHz). All data are for upwind conditions.

APPENDIX REFERENCES

A1. Rice, S.O., "Reflection of Electromagnetic Waves from Slightly Rough Surfaces," Comm. Pure and Appl. Math., 4(No. 2-3): 351-378 (1951).

A2. Bass, F.G., Fuks, I.M., Kalmykov, A.I., Ostrovsky, I.E., and Rosenberg, A.D., "Very High Frequency Radiowave Scattering by a Disturbed Sea Surface," IEEE Trans., AP-16 (No. 5): 554-568 (1968).

A3. Peake, W.H., "Theory of Radar Return from Terrain," IRE Nat. Convention Record, Vol. 7, Part 1, pp. 27-41, 1959.

A4. Wright, J W , "Backscattering from Capillary Waves with Application to Sea Clutter," IEEE Trans., AP-14 (No. 6): 749-754 (1966).

A5. Phillips, O.M., "The Dynamics of the Upper Ocean," London:Cambridge Univ. Press, 1966.

DOCUMENT CONTROL DATA - R & D

Security classification of title, body of abstract and indexing annotation must be entered when the overall report is classified

1 ORIGINATING ACTIVITY *(Corporate author)*	2a. REPORT SECURITY CLASSIFICATION
Naval Research Laboratory	Unclassified
Washington, D. C. 20022	2b. GROUP

3 REPORT TITLE

Radar Sea Return in High Sea States

4 DESCRIPTIVE NOTES *(Type of report and inclusive dates)*

This is a final report on one phase of a continuing problem.

5 AUTHOR(S) *(First name, middle initial, last name)*

J. C. Daley, W. T. Davis and N. R. Mills

6 REPORT DATE	7a. TOTAL NO. OF PAGES	7b. NO. OF REFS
September 25, 1970	50	13

8a. CONTRACT OR GRANT NO	9a. ORIGINATOR'S REPORT NUMBER(S)
NRL Problem R07-20	
b. PROJECT NO	NRL Report 7142
PO-0-0007	
c.	9b. OTHER REPORT NO(S) *(Any other numbers that may be assigned this report)*
d.	

10 DISTRIBUTION STATEMENT

This document has been approved for public release and sale; its distribution is unlimited.

11 SUPPLEMENTARY NOTES	12 SPONSORING MILITARY ACTIVITY

13 ABSTRACT

In order to obtain a more exact specification of the variation of the radar cross section of the sea with increasing sea roughness, and to determine a worst-case condition for sea clutter, NRL has conducted a high-sea-state clutter measurement program in the North Atlantic.

The processing and analysis of the radar backscatter, recorded in the North Atlantic in February 1969, have been completed. Radar return was collected on four frequencies in both linear and cross polarizations, and the normalized radar cross section σ_0 of the sea surface was obtained as a function of radar and surface parameters for the high sea states encountered. The study of the behavior of the median value of σ_0 as a function of the radar parameters and sea conditions resulted in the following conclusions at high sea states characterized by winds of 20-50 knots and wave heights of 10-26 ft: (a) the value of σ_0 is independent of wavelength for vertical polarization but maintains an inverse wavelength dependence for horizontal polarization, (b) the direct polarization ratio remains significant for all wavelengths as the sea roughness increases and is a function of wavelength, (c) the value of σ_0 is sensitive to wind direction, with consistently higher clutter observed in the upwind direction for all wavelengths and both direct polarizations, and (d) the value of σ_0 does not increase significantly with wind velocity in the region 20-50 knots, indicating that σ_0 approaches a maximum value, or "saturation," with increasing surface roughness. The high-sea-state measurement program has provided a comprehensive data bank of pulse-to-pulse returns which may be analyzed to develop statistical models of the sea clutter process.

DD FORM 1473 (PAGE 1)

S/N 0101-807-6801

14 KEY WORDS	LINK A		LINK B		LINK C	
	ROLE	WT	ROLE	WT	ROLE	WT
Radar echoes						
Radar cross sections						
Oceans						
Wind direction						
Wind velocity						